INVESTIGATION OF THE EFFECT OF SOIL STRUCTURE INTERACTION ON THE
BEHAVIOR OF CONCRETE FACED ROCKFILL DAMS AND ASSESMENT OF
CURRENT ANALYSIS METHODOLOGIES

A THESIS SUBMITTED TO
THE GRADUATE SCHOOL OF NATURAL AND APPLIED SCIENCES
OF
MIDDLE EAST TECHNICAL UNIVERSITY

BY

EMRAH ERŞAN ERDOĞAN

IN PARTIAL FULFILLMENT OF THE REQUIREMENTS
FOR
THE DEGREE OF MASTER OF SCIENCE
IN
CIVIL ENGINEERING

JUNE 2012

Approval of the thesis:

INVESTIGATION OF THE EFFECT OF SOIL STRUCTURE INTERACTION ON THE BEHAVIOR OF CONCRETE FACED ROCKFILL DAMS AND ASSESMENT OF CURRENT ANALYSE METHODOLOGIES

Submitted by **EMRAH ERŞAN ERDOĞAN** in partial fulfillment of the requirements for the degree of **Master of Science in Civil Engineering Department, Middle East Technical University** by,

Prof. Dr. Canan ÖZGEN
Dean, Graduate School of **Natural and Applied Sciences**   _____

Prof. Dr. Güney ÖZCEBE
Head of Department, **Civil Engineering**   _____

Assist. Prof. Dr. Yalın ARICI
Supervisor, **Civil Engineering Dept., METU**   _____

Examining Committee Members:

Prof. Dr. A.Melih YANMAZ
Civil Engineering Dept., METU   _____

Assist. Prof. Dr. Yalın ARICI
Civil Engineering Dept., METU   _____

Assist. Prof. Dr. Özgür KURÇ
Civil Engineering Dept., METU   _____

Assist. Prof. Dr. Nejan Huvaj SARIHAN
Civil Engineering Dept., METU   _____

Assist. Prof. Dr. Tolga YILMAZ
Engineering Science Dept., METU   _____

Date: June 21, 2012

I hereby declare that all information in this document has been obtained and presented in accordance with academic rules and ethical conduct. I also declare that, as required by these rules and conduct, I have fully cited and referenced all material and results that are not original to this work.

Name, Last name: Emrah Erşan ERDOĞAN

Signature   :   _____

ABSTRACT

INVESTIGATION OF THE EFFECT OF SOIL STRUCTURE INTERACTION ON THE
BEHAVIOR OF CONCRETE FACED ROCKFILL DAMS AND ASSESMENT OF CURRENT
ANALYSIS METHODOLOGIES

Erdoğan, Emrah Erşan
M.Sc., Department of Civil Engineering
Supervisor: Assist. Prof. Dr. Yalın Arıcı

June 2012, 64 pages

CFRD (Concrete Faced Rockfill Dam) construction becomes more frequent recently
not only because of its secure nature, but also its economical cost where its built up
material is feasible to obtain. Although CFRDs are known to be safe compared to
other dam types, it is behavior during an earthquake loading still not a well-known
aspect since it is mostly constructed in regions of low seismicity until now.

Considering this fact, this study's primary purposes are set to find the mathematical
model size of a "large" domain model to correctly simulate the Soil-Structure
Interaction (SSI) effects, to investigate the reliability of the current simulation
methods applicable to the modeling of CFRDs and to observe nonlinear performance
of CFRDs, mainly focusing on the performance of the face slab. Results of this study
clearly state an adequate model size to simulate the SSI effects correctly using the
finite element method with the help of the previous studies. The change of the
response of the dam depending on the dam and underlying soil moduli and depth is
presented clearly. Besides the testing of the performance of a simplified model, the
reliability of this approach is judged and found to be not accurate enough when

compared to theoretically "exact" results. Crack occurrence on the face slab during a non-linear analysis is presented, its importance is discussed both in magnitude and pattern. A significant spreading of cracking after an earthquake loading is observed.

Keywords: Concrete Faced Rockfill Dam, Soil Structure Interaction, Crackwidth, Earthquake, Finite Element Analysis.

ÖZ

YAPI ZEMİN ETKİLEŞİMİNİN ÖN YÜZÜ BETON KAPLI KAYA DOLGU BARAJLARIN
DAVRANIŞINA ETKİSİNİN İNCELENMESİ VE GÜNÜMÜZDE KULLANILAN ANALİZ
METHODLARININ DEĞERLENDİRİLMESİ

Erdoğan, Emrah Erşan
Yüksek Lisans, İnşaat Mühendisliği Bölümü
Tez Yöneticisi: Yrd. Doç. Dr. Yalın Arıcı

Ön yüzü beton kaplı kaya dolgu barajların günümüzde giderek artan bir sıklıkta kullanılmaya başlanmasındaki temel sebep yalnızca doğası gereği güvenli oluşu değil, aynı zamanda temel yapı malzemelerinin elde edilişinin mümkün olduğu yerlerde yapım maliyetlerinin oldukça ekonomik oluşu olarak da gösterilebilir. Bu barajlar her ne kadar diğer tiplere göre daha güvenli olarak değerlendirilse de, şimdiye kadar çoğunlukla düşük sismik hareketin bulunduğu bölgelerde inşa edilmiş olduklarından deprem yükü altındaki davranışı hala tam olarak anlaşılabilmiş bir kavram değildir

Bu durum dikkate alınarak, bu çalışmanın temel amaçları Yapı Zemin Etkileşiminin etkisini doğru olarak simüle edecek 'büyük' modelin matematiksel model büyüklüğünü bulmak, ön yüzü beton kaplı baraj modellemesine uygulanabilir mevcut simülasyon metodlarının güvenilirliğini değerlendirmek ve ağırlıklı olarak ön yüz kaplamanın performansı olmak üzere barajın doğrusal olmayan uzaydaki

performansının gözlemlenmesi olarak belirlenmiştir. Bu çalışmanın sonuçları, Yapı Zemin Etkileşimi etkilerini yeterli bir biçimde simüle edecek sonlu elemanlar yöntemi ile oluşturulmuş model büyüklüğünü açıkça belirtmektir. Yapı tepkilerinin baraj ve zemin elastisite modülüne ve zemin derinliğine göre değişimi açık bir şekilde sunulmuştur. Ayrıca basitleştirilmiş bir modelin performansı test edilmiş, metodun güvenilirliği değerlendirilmiş ve alınan sonuçlar kati sonuçlarla karşılaştırıldığında yeterince hassas olmadığı bulunmuştur. Doğrusal olmayan analiz esnasında ön yüz betonundaki çatlak oluşumu sunulmuş, bu durumun önemi hem büyüklük hem de şekil açısından tartışılmış ve deprem yükü sonrasında ciddi bir yayılım gözlemlenmiştir.

Anahtar Kelimeler: Ön Yüzü Beton Kaplı Kaya Dolgu Baraj, Yapı Zemin Etkileşimi, Çatlak Genişliği, Deprem, Sonlu Elemanlar Metodu Analizi.

To My Family

ACKNOWLEDGEMENT

TABLE OF CONTENTS

LIST OF TABLES

TABLES

LIST OF FIGURES

FIGURES

LIST OF SYMBOLS / ABBREVATIONS

a_0 & a_1	Rayleigh Damping Parameters
b_0, b_1, b_2 & b_3	Equation Constants
ASCE	American Society of Civil Engineers
ASTM	American Society for Testing and Materials
B	Base Width
BEM	Boundary Element Method
C	Damping Matrix
CFRD	Concrete Faced Rockfill Dam
D	Depth of the Soil
E	Young's Modulus
E_d	Young's Modulus of the Dam
E_f	Young's Modulus of the Foundation
EoI	End of Impoundment
A_c	Effective Area of the Concrete Surrounding Each Bar
d_c	Distance from the Extreme Tension Member to the Center of the Closest Bar
f_1 & f_2	Yield Surfaces
f_c	Compressive Strength of Concrete
f_t	Tensile Strength of Concrete
f_y	Yield Strength of Steel
f	Maximum Frequency of Interest
FEM	Finite Element Method
g_1 & g_2	Plastic Potential Surfaces
G	Shear Modulus
G_c	Compressive Fracture Energy
G_f^I	Mode-I Fracture Energy
G_{ref}	Reference Tangent Shear Modulus
GPa	GigaPascal
H	Height of the Dam
H_f	Height of the Foundation
Hz	Hertz
K	Stiffness Matrix
K_{ref}	Reference Compression Modulus

l	Maximum Edge Length
m	Floating Point Value
m	Meter
M	Mass Matrix
MPa	MegaPascal
MSE	Mean Squared Error
$\Delta p'$	Pressure Shift for the Shear Yield Surface
p'	Mean Effective Stress
p_a	Atmospheric Pressure
p_c	Pre-consolidation Pressure
p'_t	Compression Offset
q'	Effective Deviatoric Stress
R	6x6 Matrix Used in Rockfill Formulation
s	Second
SSI	Soil-Structure Interaction
t_n	Normal Traction
t_t	Tangential Traction
t	Ton
u	Displacement
$\dot{u}$	Velocity
$\ddot{u}$	Acceleration
$u_\Im$	Imaginary Part of the Displacement
$u_\Re$	Real part of the Displacement
$\ddot{u}_g$	Ground Acceleration
USACE	U.S. Army Corps of Engineers
V_S	Shear Wave Velocity
w	Frequency of Interest in Hertz
w1	Fixed Base First Fundamental Frequency
w	Direction of Integration Analogous to z Direction
$\dot{\text{w}}$	Velocity in w Direction
w_{max}	Maximum Crack Width
$\tan\phi_1$	Friction Coefficient
$\tan\vartheta_1$	Tangent of the Angle of Dilatancy
δ	Elasticity Reduction Factor
$\alpha\ \&\ \beta$	Parameters for the Dynamic Backbone Function
β_{sg}	Coefficient Accounting for Strain Gradient
ϕ	Friction Angle
ϕ_{cv}	Friction Angle at a Constant Volume
$\Delta\kappa_1\ \&\ \Delta\kappa_2$	Internal Parameters
ρ	Material Density
τ_{xy}	Shear Stress
γ	Hysteretic Damping Factor
γ_{xy}	Shear Strain

γ_r	Reference Shear Strain
$\dot{\lambda}$	Multiplier for Interface Constitutive Model
$\Delta\gamma^p$	Equivalent Plastic Deviatoric Strain Increment
ε_y	Yield Strain of Steel
ε_v^p	Volumetric Plastic Strain
ε_{scr}	Strain in Reinforcing Bar at Crack Location
Ω	Solution Frequency
$\zeta \& \eta$	Local Element Axes
ξ	Damping Ratio
$\xi_{\max}$	Maximum Damping Ratio
υ	Poisson's Ratio
ϑ	Angle of Dilatancy
ω	Circular Frequency of Interest
σ	Normal Stress
λ	Estimator
$\hbar$	Estimation
ψ	Incident Angle
θ	Lode's Angle

CHAPTER 1

INTRODUCTION

1.1. Dam Construction

Dams can be defined as impervious barriers constructed across a waterway to divert and control the water flow for the benefit of the mankind. Construction of dams is one of the oldest technical activities applied for the benefit of the societies.

Dams made of soil and rock has been known since the ancient times. Our knowledge about the ancient dam construction shows that there were over 30 dam structures made of earth materials existing in the beginning of our civilization history [1] which served for irrigation purposes or to form water supplies. The usage of earth materials in dam construction was preferred throughout the history since the material used is usually easily obtainable. On the contrary, in the history of modern dam construction, most of the early dams were made of concrete since appropriate earth moving equipment was developed much later.

However, development of earth moving equipment did not only ease the earth dam construction but also leaded to another invention named as rockfill dams with the help of increasing knowledge of soil behavior. Since then rockfill dam construction practice has evolved rapidly from dumped rockfill dams to well-engineered compacted rockfills having imperious face or earth cores.

1.2. History of Rockfill Dam Construction

Although rock, as a construction material, was used in dam construction starting from the ancient times, the modern rockfill dam is considered to be a product of the California gold rush. The miners of the California Sierras used rockfill dams to store water for dry season sluicing of placer ore deposits with the knowledge of blasting and availability of rock [2].

In these early stages of rockfill dam construction, constructed dams were mainly timber faced, dumped rockfills up to 25 m height with very steep slopes (0.5:1 to 0.75:1) [2]. As the trend continues, dumped rockfill dams started to be built with heights exceeding 100 m and having an impervious face mainly made of concrete (CFRD), a notable example can be considered as the Salt Springs Dam in California (101 m). In parallel with this trend, in ASCE Symposium on rockfill dams in 1939, a rockfill dam was defined as, "A dam consisting of loose (dumped) rockfill with slopes on both faces closely approximating natural slopes, with an impervious facing on the upstream side between which and the rockfill there should be placed a cushion dry rubble" [3].

In the mid period of the 20th century, as knowledge accumulated on rockfill dam performance, previous practices encouraged the designers to construct higher rockfill dams. However dams constructed between years 1950-1960 experienced serious leakage problems with serious face damage which led to a temporary suspension in rockfill dam construction, since the settlements after the reservoir loading started to become too large.

Rockfill compressibility was a major limitation to overcome the large settlement problem, since traditional approach was to use large size rock with high compressive strength which passes ASTM specifications for concrete aggregate [2]. This design approach was not only limited the designers to construct a rockfill dam with a moderate height but also restricted them to construct rockfill dams to the locations where suitable a high-strength rock was available. With the increasing

demand to construct higher rockfill dams and the advent of vibratory roller equipment, transition from dumped to compacted rockfills was inevitable.

Traditional approach was abandoned and rockfills were started to be compacted in thin layers usually supplemented by the application of water, reducing the post-construction settlements drastically. This breakthrough made the rockfill dam construction adaptable also to areas having locally available weak rock. Thus, CFRD construction became more economical as compared to other alternatives, since it was not possible to find appropriate clayey material to form an impervious core [2].

Since then, CFRD construction has became quite popular and has been used with increasing frequency because of the fact that it is found to be the least-cost alternative selection in places where their built-up material is feasible to obtain.

With the increased feasibility, CFRDs have improved the living conditions of the societies they serve for so many years. But like any men made structure they constitute many dangers for the environment and the living forms live in it, besides the benefits they provide.

1.3. CFRD Safety Considerations

CFRDs are widely believed to be the one of the safest types among the alternatives for dams. Many risks that could threaten other types of dams are usually not considered as a serious danger factor in CFRDs.

1.3.1. Failure Due to Overtopping

Perhaps one of the most advantageous aspects of a CFRD can be considered to be their ability to withstand passage of flood water through the uncompleted structure [2]. In a water flow condition through the body of the dam, since a modern CFRD has less leakage and good permeability at the dam base, it could withstand this unexpected water flow easily. However, water flow over the superstructure is another concern. Although the same properties have a positive effect, a reinforced rockfill is usually necessary to make the rockfill lifts withstand this unexpected

condition [4]. Post-construction overtopping can be controlled by both of the above properties with the help of an adequate spillway design.

1.3.2. Failure due to Slope Instability

Since CFRDs have a good permeability and usually a gentle slope (1.0 to 1.3H or 1.0 to 1.4H), it is easy to maintain its stability if the leakage can be prevented properly.

1.3.3. Failure due to Bearing Capacity

With a gentle slope CFRD's have broad bases as compared to a concrete gravity dam similar in height, thus imposing lower stresses to the ground and reducing the bearing capacity failure risk to minimum. This also makes them feasible to be constructed even on weak foundations without any major improvement.

1.3.4. Failure due to Poor Structural Design

The built-up materials that are used in rockfills are usually highly plastic materials that can accommodate large deformations under severe loading conditions. With a proper face slab design and a built-up material that has adequate strength and plasticity, the strength reduction due to pore water pressure can be prevented by controlling leakage. It also has lower structural standards as compared to a concrete dam, since concrete dams can accommodate quite low strains compared to CFRDs.

However due to their nature as permanent structures, CFRDs have to resist all loading conditions during and after its service life. Although previously given discussions are believed to be true, they are mainly based on previous experiences and analytical studies conducted for CFRDs which were constructed in regions with low seismicity.

According to Seed [5], "Two rockfill dams (Milboro earth core rockfill-128 m, Cogoti concrete face rockfill-84 m) have withstood moderately strong ground shaking with no significant damage, and if the rockfill is kept dry by means of concrete facing they should be able to withstand extremely strong shaking with only small deformations".

Parallel to this judgment, many engineers in the dam construction practice have argued that CFRDs are inherently safe against potential seismic damage mainly because; [6]

- The whole CFRD superstructure is dry by means of an impervious facing, making the earthquake effect unable to raise the pore water pressure which causes strength degradation during earthquake loading, and loss of strength due to the weakening of rock particles in the long term.
- Reservoir water pressure acting on the upstream face makes the rockfill to act in the benefit of structural stability.

Hence, there has been little attention on the design features of a modern compacted CFRD in seismic regions. However, most of the judgments made previously depend on the assumption that the dam body is kept dry during and after the shaking. However opening of contact surfaces and the damage on the face slab increases the leakage of reservoir water, which makes the body wet and degrades the strength. This condition may lead to accumulation of structural damage that can generate high maintenance costs in the lifetime of the dam or even cause a structural failure.

In addition, the structural response is known to be affected directly by the soil deposit that lies beneath the dam. In terms of static loading the effect is limited to the stiffness properties of the deposit and mostly how much it settles after the load is applied. However in terms of dynamic loading, like a seismic loading, the effects are harder to quantify. Soil deposit determines how the ground motion travels before and after hitting the structure which can have entirely different dynamic properties depending on the soil type it rests on. Even though these aspects are not taken into consideration in current design practice of CFRDs, to correctly simulate the dynamic behavior these effects, widely known as soil-structure interaction (SSI), should also be addressed properly.

The recent experience from the Wenchuan earthquake (2008), in which a major CFRD system was moderately damaged [7], also indicates the importance of the correct simulation of the dynamic behavior of CFRDs.

1.4. Dynamic Behavior of Dams

As mentioned above, SSI effects have a critical role on dynamic behavior of the structures. In this regard, several studies are conducted in past years to correctly simulate the effect of SSI on dams, mainly concrete gravity dams. As the major concern of an SSI analysis is the simulation of a non-reflecting model boundary, the main issue covered in these studies has been the correct definition of boundary conditions while considering SSI. A concise summary of previous work on dynamic analyses of dams with a focus on SSI is provided in the following paragraphs.

1.4.1. Previous Studies on the Effects of SSI on Dams

Several studies on SSI were conducted with primary focus on the nuclear structures in the second half of the twentieth century. The most prominent works on the effect of SSI on concrete dams, currently in wide spread use in the design of such structures, are the studies by Fenves & Chopra [8] and Medina et al. [9]. Common feature of these studies is that these are response studies conducted in frequency domain, thus limiting the results and recommendations in linear sense.

The simplified method proposed by Fenves & Chopra [8] is based on the assumption that the contact surface between the concrete dam and the soil behaves rigidly, and the dam superstructure rests on an elastic 2-dimensional infinite medium. A single degree of freedom system can be considered to represent the dam structure with an equivalent damping value and natural vibration frequency. The major assumptions in Fenves & Chopra [8]'s method can be summarized as below:

- Concrete gravity dams are modeled in a 2-dimensional space and the contribution of the first vibration mode to the overall response is quite high.

In this sense it is substantially advantageous to consider these dams as single degree of freedom systems.

- Complex natural vibration modes are neglected by expressing a rigid contact surface behavior.

- It is quite essential to express the soil medium as an elastic material since a frequency domain solution is required.

- Soil medium beneath the dam superstructure is idealized as an infinite medium to make it possible to obtain a closed form exact solution.

A finite element based model is also proposed [10] based on the implementation of the studies outcomes. The serious disadvantages of the assumptions provided above are:

1) The method is a realistic approach only if the first modal response is dominant in the considered system. Since any change in the dam type & geometry can change contribution of the first fundamental mode, use of the method in systems with different geometries should be done with caution.

2) Since the soil beneath the dam is considered as an infinite medium, soil properties beneath the dam superstructure are assumed to be constant and/or there is no stiff rock in a considerable depth. That kind of a constant featured semi-infinite soil medium prediction is quite unrealistic since soil properties could vary along the depth and/or there could be a stiff rock formation in a shallow depth.

3) Frequency based methods do not permit nonlinear solutions for both the dam and the soil.

A significant number of dams are built on layered soils, where an infinite half space assumption cannot be made. The approach to the SSI problem for a layered medium, by Medina et al. [9] using 'Boundary Element Method' (BEM), considers the dam as a triangular shaped structure on a layered strata underlain by stiff rock. The structure is considered as a multi degree of freedom system and contact behavior is defined as flexible. Thus, all vibration modes are taken into consideration. However, since it is not practical to employ a BEM analysis for design,

the method proposed by Fenves & Chopra [8] is widely used in practice to simulate SSI effects due to its simplicity.

Both of above approaches are in the frequency domain limiting the response to linear behavior. Since the response of a dam is expected to be nonlinear to some extent and some damage to structures are allowed in modern design techniques, a nonlinear modeling considering the SSI and plasticity effects in time domain is required. Such a model in time domain can be obtained with the use of proper boundary conditions known as local boundaries in time history analyses.

1.4.2. Local Boundaries in General

Many early analytical studies were conducted to simulate sonic flow. These studies mainly considered the problem as a wave propagation problem in an infinite solid. This approach resulted in many closed form solutions by simplifying the problem to simple homogeneous systems. However, most of the problems encountered in practice have more complicated geometries and it is nearly impossible to find such closed form solutions for these systems.

Using finite medium to express flow in infinite domain is a complex task. Main problem of these type of simulations is how to define the boundaries of the proposed models to form boundaries referred as an absorbing, silent, non-reflecting or transmitting boundary, that do not reflect propagating waves within a medium. A number of different boundary formulations were proposed to be used in discrete methods such as the finite element and finite difference schemes. Thus, it became possible to obtain accurate solutions to some SSI problems through FE models since the behavior of these boundaries and their effect on the whole model produce equivalent results as compared to an infinite succession of finite element beyond the edges of the model, which also makes them consistent in these cases [11]. Consequently, they became particularly useful and essential in studies of SSI effects [12-14].

However, it is not always that easy to decide which boundary to use while forming a mathematical model. Kausel [11], argued that although they all seem to be significantly different from each other in conceptual basis, numerical implementation and mathematical formulation, in reality they are all mathematically related and are comparable in performance. He tested the most popular ones; as Lindman-Engquist-Majda [15] [16], Lysmer-Kuhlemeyer [17], Ang-Newmark [18], Modified Smith [19] and Liao-Wong [20], and found that when it comes to performance Lindman-Engquist-Majda and Liao-Wong are the most convenient ones to be used in finite differences and finite elements applications respectively [11]. He also noted that these boundaries are not that easy to implement and dynamically unstable in high frequency excitations. In practice, however, usually ease of implementation determines which method to be used. In this manner, above mentioned convenient boundaries do not seem to be applicable in most cases.

Implementation difficulties make these boundaries not preferable in commercial programs, thus precluding the use of these methods in practical applications. According to Kausel [11], easiest one to implement is Lysmer-Kuhlemeyer [17] boundary, also referred as viscous boundary. This boundary also does not have the same dynamic instability problem in high frequencies and can safely be used as a boundary condition while constructing a model that simulates sonic flow.

1.5. Scope of this Study

The focus of this study can be divided into 3 main topics which can be summarized as;

- Determination of the adequate model size to correctly simulate SSI effects on CFRDs
  - To see the changes in response amplitudes with the soil-structure interaction effects.
  - To see the changes in dynamic properties with the soil-structure interaction effects.

- Investigation of the reliability of the current simulation methods applicable to the modeling of CFRDs, while keeping the main focus on the SSI effects.
  - ➢ To assess the performance of the mathematical models that is currently used in practice in the design of CFRDs.
  - ➢ To assess if current design practices are over or under conservative.

- To observe the CFRD non-linear performance during a strong shaking on different foundations.
  - ➢ To see the performance of the face slab during an "Operation Based Earthquake "(OBE).

To describe the efforts which make it possible to reach the goals listed, this document is divided into the following chapters with the contents that are mentioned in the following paragraphs.

Chapter 2 mainly deals with the material models used in this study. CFRD system is explained in detail and all calibrated constitutive models and boundary conditions are described.

In Chapter 3; model features are decided that simulate the real linear CFRD behavior using the outcomes of the previous studies. Since modeling philosophies have to be decided while forming a mathematical model that simulates these effects on CFRDs, outcomes of the study conducted by Medina et al. [9] is used to calibrate the mathematical models used. Then current analyses procedures are investigated and the responses of these models and the real solution that considers the effect of SSI are compared.

In Chapter 4; a realistic CFRD system is modeled by taking into consideration the SSI effects and keeping hydrodynamic effects out of scope, to be able to observe the site effects properly. Forming of the cracks and axial stresses in the face slab, top displacement of the crest and acceleration responses along the model are studied with proper care.

Finally, Chapter 5 contains a brief summary of the whole study, the conclusions obtained and the suggestions for possible future work.

CHAPTER 2

MATERIAL MODELING

2.1. Introduction

In this chapter of the study, the material models used in the modeling of the CFRD system are explained in detail. Calibrated material models are taken from a study on CFRD face plate cracking [21].

Dam body consists of the reinforced concrete face slab, rockfill, plate-cushion layer interface and plinth. The plinth-face slab connection was simulated using an interface model defined to simulate the separation behavior between face slab and the plinth at the cold joint at this location.

Soil layer that lies beneath the superstructure is modeled as a linear elastic material with non-reflecting boundary conditions at sides. To achieve this non-reflecting condition viscous boundaries are used. Theoretical background of this boundary is also explained in detail.

2.2. Face Slab

The face slab, made of reinforced concrete, is modeled using two different material models. The constitutive model for concrete is based on total strain fixed crack model. The compressive crushing behavior is modeled by using a parabolic curve based on compressive fracture energy G_c, to make the model mesh independent

and objective, and compressive strength f_c. The tensile behavior is modeled by using a linear softening function beyond the tensile strength f_t with the ultimate tensile strain based on mode-I fracture energy G_f^I [22]. Mentioned tensile and compressive constitutive relations are given in (Figure 2.1), where h is defined as the effective element size. Material model for reinforcement is chosen as a typical strain hardening diagram as shown in Figure 2.1, where f_y and ε_y are the yield strength and strain respectively [21].
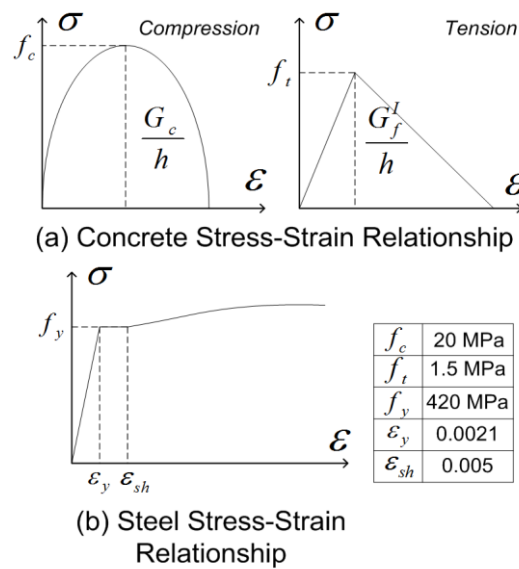
Figure 2.1. *Constitutive Model for Face Slab [21]*

2.3. Rockfill

Rockfill was modeled by utilizing two material models which simulate the behavior under static and dynamic loading respectively, which does not account for particle breakage of rockfill. Since there are no well-documented test results available for the dam materials for the case study of interest, outcomes of a triaxial testing program conducted on rockfill specimens are assumed to represent the static behavior [23]. This study shows that;

- The stress-strain behavior of the rockfill materials is nonlinear, inelastic and stress dependent.

13

- An increase in confining pressure tends to increase the value of peak deviatoric stress, axial strain and volumetric strain at failure.
- An increase in the size of the particles results in an increase in volumetric strain at the same confining pressure.

Modified Mohr-Coulomb formulation by Groen [22][24] is used in order to capture the shear and volumetric deformation of rockfill and account for the dependency of material properties on confinement. This constitutive relation utilizes a yield surface which has a double hardening-softening model in which shear and compression failures are uncoupled (Figure 2.2). In p'-q' space, shear and compression failure surfaces can be defined as in equations given below:

$$f_1 = \frac{q'}{R_1(\theta)} - \frac{6\sin\phi}{3-\sin\phi}(p'+\Delta p') = 0 \tag{2.1}$$

$$R_1(\theta) = \left(\frac{1-\beta_1\sin 3\theta}{1-\beta_1}\right)^{-0.229} \tag{2.1a}$$

$$\beta_1 = \left(\frac{3+\sin\phi}{3-\sin\phi}\right)^{1/0.229} - 1 \left/ \left(\frac{3+\sin\phi}{3-\sin\phi}\right)^{1/0.229} + 1 \right. \tag{2.1b}$$

$$f_2 = (p'+\Delta p')^2 + \frac{2}{9}q'^2 - p_c^2 = 0 \tag{2.2}$$

where;

ϕ =Friction angle

q' =Effective deviatoric stress

p' =Mean effective stress

$\Delta p'$ =Pressure shift for the shear yield surface

p_c =Pre-consolidation pressure

θ =Lode's angle

The evolution of the shear failure surfaces is governed using the multi-linear variation of the sine of the friction angle with respect to the change in an internal model variable (Figure 2.2), $\Delta\kappa_1$ (2.3), whereas the evolution of the compression

failure surfaces is governed using the change in the pre-consolidation pressure with respect to the change in an another internal variable, $\Delta\kappa_2$ (2.4).

$$\Delta\kappa_1 = \sqrt{\left(\frac{2}{3}\right)\left(\Delta\gamma^p\right)^T R\left(\Delta\gamma^p\right)}$$
(2.3)

$$\Delta\kappa_2 = -\Delta\varepsilon_v^p$$
(2.4)

where;

$\Delta\gamma^p$ = Equivalent plastic deviatoric strain increment

R = 6x6 factor matrix used in rockfill formulation

ε_v^p = Volumetric plastic strain

(a) Shear and Compression Yield Surfaces in p'-q' Space

(b) Multi-Linear Hardening of Friction Angle w.r.t. Internal Variable κ_1
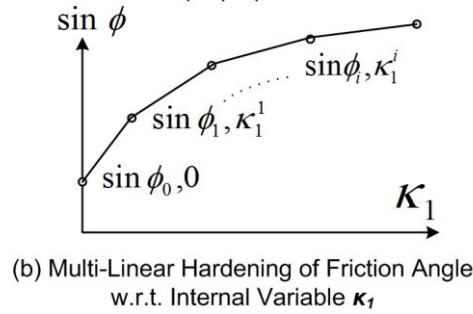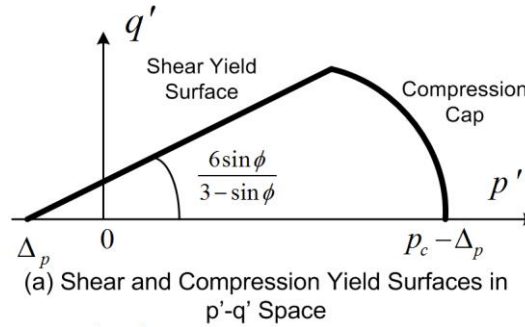
Figure 2.2. *Modified Mohr-Coulomb Plasticity Model [21]*

Post-yield inelastic strain rate is determined by the plastic potential surfaces given in (2.5, 2.6).

$$g_1 = q' - \frac{6\sin\vartheta}{3-\sin\vartheta}(p'+\Delta p')$$
(2.5a)

$$\sin\vartheta = \frac{\sin\phi - \sin\phi_{cv}}{1-\sin\phi\sin\phi_{cv}}$$
(2.5b)

$$g_2 = (p' + \Delta p')^2 + \frac{2}{9}q'^2 - p_c^2 \qquad\qquad\qquad (2.6)$$

where;

ϕ_{cv} =Friction angle at a constant volume

Within the failure surfaces a nonlinear elastic behavior is employed by the use of power law where it is assumed that the compression modulus (K_t) is power of a current pressure (2.7).

$$K_t = K_{ref}\left(\frac{p' + p'_t}{p_a}\right)^{1-m} \qquad\qquad\qquad (2.7)$$

where;

p'_t =Compression offset

p_a =Atmospheric pressure

K_{ref} =Reference compression modulus

m =Model parameter

This constitutive model is calibrated to tri-axial tests conducted at three levels of confining stress using the deviatoric stress-axial strain and volumetric strain-axial strain results (Figure 2.3) as given in previously mentioned study [23]. Calibrated model parameters are presented in (Table 2.1) [21].
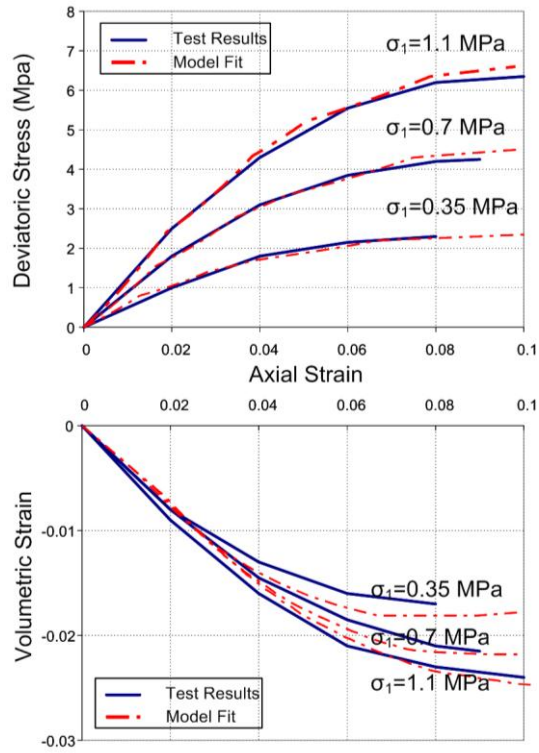
Figure 2.3. *Constitutive Rockfill Plasticity Model Performance [21]*

Table 2.1. *Parameters for Rockfill Plasticity Model [21]*

Parameter	Value
p'_t	0.2*
$\Delta p'$	0.02*
p_c	1.5*
K_{ref}	13.3*
m	0.22
$\sin\phi(\kappa_1^i)$	0.52(0.00)/0.66(0.007)/0.70(0.014)/0.74(0.036)/0.90(0.44)
$\sin\phi_{cv}$	0.755
υ	0.32

To define the dynamic behavior, a modified Ramberg-Osgood formulation (2.8) is used to simulate stiffness degradation (2.9) and hysteretic damping of the rockfill material dependent on the level of cyclic strain.

$$\gamma_{xy} = \frac{\sigma_{xy}}{G}\left(1 + \alpha\left|\tau_{xy}\right|^{\beta}\right)$$ (2.8a)

$$\alpha = \left(\frac{2}{\gamma_r G}\right)^{\beta} \quad \& \quad \beta = \frac{2\pi\xi_{max}}{2 - \pi\xi_{max}}$$ (2.8b)

$$G = G_{ref}\left(p'/p_a\right)^{0.5}$$ (2.9)

where;

γ_{xy} =Shear strain

$\alpha \,\&\, \beta$ =Parameters for dynamic backbone function

G_{ref} =Reference tangent shear modulus

γ_r =Reference shear strain

ξ_{max} =Maximum damping value

Reference shear strain value ($\gamma_r = a\exp(bp')$) is defined as a function of the mean stress p' at the End of Impoundment (EoI) stage to represent the dependency of the damping ratio and stiffness degradation on the confining stress [26][26][27]. Logarithmic regression on γ_r values are calibrated to the existing backbones and damping ratio curves at three confinement levels as given in Figure 2.4 and the parameters $a \,\&\, b$ are obtained as 0.0038 and 0.0040 respectively [21]. Since Ramberg-Osgood formulation provides very small damping values at very small shear strains, an additional 2% viscous damping is assigned to the constitutive model using Rayleigh damping assumption (2.10).

$$C = a_0 M + a_1 K$$ (2.10)

where;

C =Damping matrix

K =Stiffness matrix

M =Mass matrix

$a_0 \,\&\, a_1$ =Rayleigh damping parameters

This addition make the shear strain vs. damping ratio curves lie in between the results for Oroville [27] and Changheba Dam [26] rockfill material. Dynamic

backbone for the shear stress-strain relationship is assumed to close to the static backbone of the subject material [23] since testing is conducted for monotonic loading only. As can be seen from Figure 2.4 a relatively good fit is obtained until $\gamma_r = 0.02$.
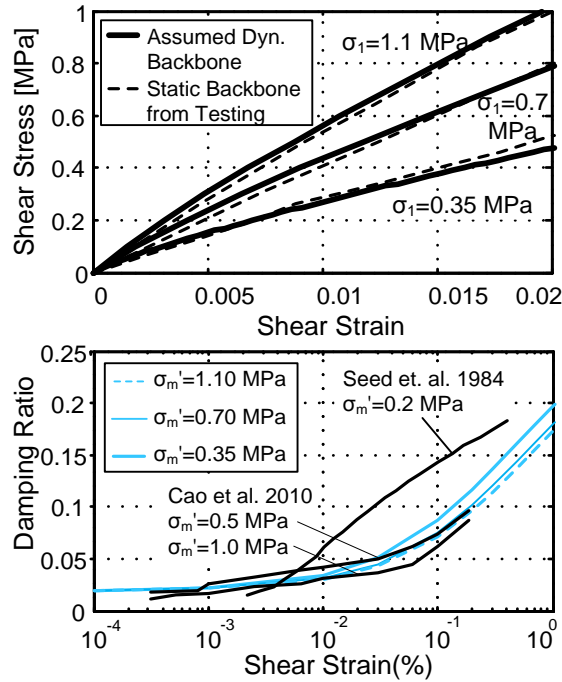
Figure 2.4. *Constitutive Rockfill Model Performance in Dynamic Loadings [21]*

2.4. Interface

Monotonic and cyclic tests conducted on the interface behavior of CFRDs [28] lead to the conclusion that the failure of the interface is a combination of both contact and filler failure, where residual friction coefficients ranging between 0.6 and 0.8 were obtained. In a separate study conducted on a concrete slab and gravel cushion layer, behavior is found to be dominated by friction with volumetric dilation [29]. Considering the outcomes of these studies, interface between the slab and the cushion layer is assumed to be governed by frictional behavior and is modeled using a simple Mohr-Colulomb plasticity model [22][30]. This model uses the following yield and plastic potential surfaces.

$$f_1 = \sqrt{t_t^2} + t_n \tan\phi_1 - c_1 = 0 \tag{2.11}$$

$$g_1 = \sqrt{t_t^2} + t_n \tan\vartheta_1 \tag{2.12}$$

where;

$\tan\phi_1$ =Friction coefficient

$\tan\vartheta_1$ =Tangent of the angle of dilatancy

t_t =Tangential traction

t_n =Normal traction

Rate of the plastic displacements, $\Delta\dot{u}^p$, is governed by:

$$\Delta\dot{u}^p = \dot{\lambda}\frac{\partial g}{\partial t} \tag{2.13}$$

where;

$\dot{\lambda}$ =model multiplier

The tangent stiffness matrix is unsymmetrical if the friction angle is not equal to the dilatancy angle ($\phi \neq \vartheta$). Mentioned constitutive model is calibrated to the test results given in [29] for a concrete-gravel layer contact (Figure 2.5) [21]. As can be seen except the later stages of sliding where the dilation is overestimated the agreement is quite reasonable.
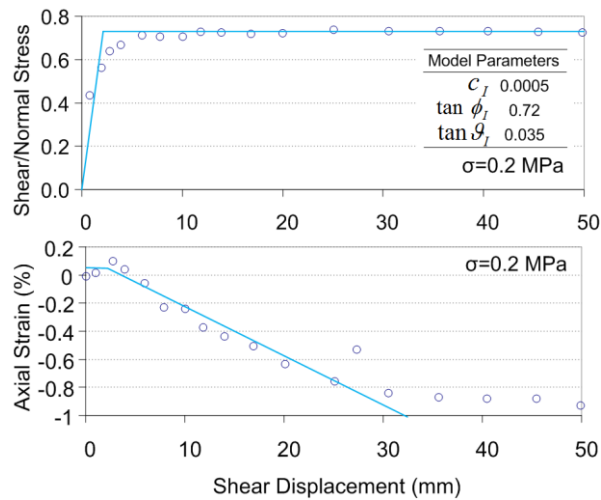
Figure 2.5. *Constitutive Interface Model Performance [21]*

2.5. Lysmer-Kuhlemeyer (Viscous) Boundary

Theoretical background of Lysmer-Kuhlemeyer boundary basically rests on the observation that stresses formed by the effect of plane waves are directly proportional to the velocities at the same location (2.14). Detailed derivation of the given equation can be found in [17].

$$\left(\tau_{xy} + \rho V_S \cos\psi \, \frac{\partial u}{\partial t} \right) = 0 \tag{2.18}$$

where;

u =Displacement

V_S =Shear wave velocity

τ_{xy} =Shear stress

ρ =Material density

ψ =Incident Angle

So, by the application of the viscous dashpots with constants equal to ρV_S at the boundaries all incident waves will be absorbed where ψ =0 (Figure 2.6).
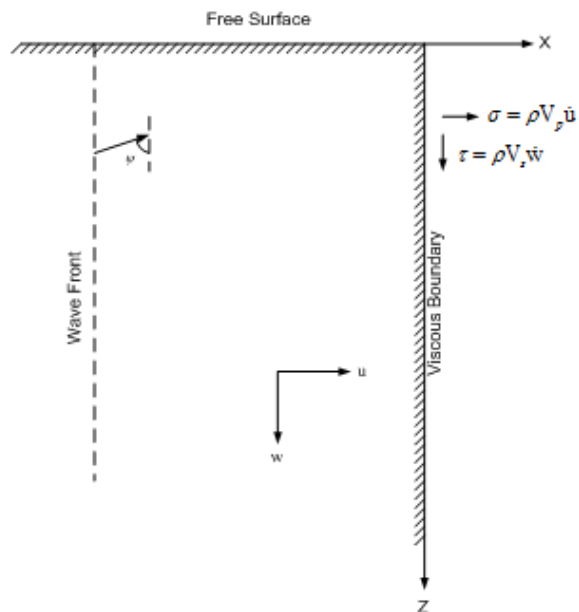
Figure 2.6. *Rayleigh Wave Absorption [17]*

21

This first order solution works pretty smooth in the longitudinal and transverse directions. However it starts to lose its absorption power as the angle of inclination to the wave front differs and is known to lose stability in static or quasi-static loadings [11].

Its applicability is quite high as compared to other proposed methods even considering the fact that proposed boundary is the very first of its kind. Although Lysmer-Kuhlemeyer boundary is not as convenient as Liao-Wong boundary, its high applicability, presence of very well defined and tested modeling principals in previous studies and availability in most of the commercial finite element based computer programs makes it a good selection among the alternatives.

In addition to its stated advantages above, it can be used also in nonlinear analysis, the boundary conditions explained in this subchapter is also selected as the non-reflecting boundary type that is used in this study and applied to the side boundaries of the models with the help of "viscous dashpots". Although modifications to this boundary by subsequent researchers have been applied, these alterations are not taken into consideration since there is no significant change in the performance of the boundary [31].

2.6. Soil Layer

Soil layer of the system is modeled as a linear elastic material as stated previously. Two different types of damping used for soil layer throughout the study, namely as hysteretic and Rayleigh damping. A frequency independent, stiffness proportional hysteretic damping (2.15) is used in the analyses conducted in frequency domain (2.16) to keep the damping ratio constant at 5% among the whole frequency range.

$$M\ddot{u} + K(1+i\gamma)u = -M\ddot{u}_g \tag{2.15}$$

$$\begin{bmatrix} K - \Omega^2 M & +K\gamma \\ -K\gamma & K - \Omega^2 M \end{bmatrix} \begin{bmatrix} u_{\Im} \\ u_{\Re} \end{bmatrix} = \begin{bmatrix} 0 \\ -M\ddot{u}_g \end{bmatrix} \tag{2.16}$$

where;

γ =Hysteretic damping factor

Ω =Solution frequency

u =Displacement

$\ddot{u}$ =Acceleration

$\ddot{u}_g$ =Ground acceleration

$u_\Im$ =Imaginary part of the displacement

$u_\Re$ =Real part of the displacement

On the other hand Rayleigh damping is used in time-domain analyses where the non-linear performance of the CFRD system is assessed. Damping ratio (2.17) is kept close to 5% within the important fundamental frequency range of the whole systems and evaluated individually corresponding to the systems dynamic properties.

$$\xi = \frac{a_0}{2}\frac{1}{\omega} + \frac{a_1}{2}\omega \qquad (2.17)$$

where;

ξ =Damping ratio

ω =Circular frequency in interest

It should also be noted that to make the whole model work properly, mesh density in the models, where viscous dashpots are used, is determined according to the recommendations made by Lysmer, who states that in order to correctly simulate sonic flow and to make the model work with the same efficiency in different frequencies, element edge lengths 'l' have to be changed depending on the shear wave velocity of the soil deposit. The ratio in (2.18) is recommended by Lysmer to calculate this maximum edge length [17]. Although the recommended ratio for is 1/12, a higher ratio of 1/8 is used in the analyses since there are no significant changes observed in the results in practice.

$$\frac{lf}{V_s} \qquad\qquad (2.18)$$

where;

l =Maximum edge length

f =Maximum frequency in interest

CHAPTER 3

ASSESMENT OF THE USE OF USACE ANALYSES METHODOLOGY USING SOIL-STRUCTURE INTERACTION EFFECTS

3.1. Introduction

In this chapter of the study, first the required domain size to effectively model the SSI effects is investigated comparing exact analytical solutions with finite element solutions in the frequency domain. As the exact analytical solutions, with BEM Medina et al. [9] or Fenves & Chopra [8] cannot be employed in nonlinear analyses, the determination of the model domain to be used in finite element model with nonlinear components is necessary. The domain size required for accuracy in modeling wave propagation effects points out to the need of a very large model in finite elements, even in a 2D setup. On the other side of the modeling spectrum, there lies the so-called USACE model, in which the dam is modeled on a massless foundation, roughly 1.5 times the dam height in dimensions at each side, significantly reducing the DOF to be used in the FE model. As the nomenclature implies, this method is based on the suggestion in the USACE [10] that is suggested in order to approximate the SSI effects on gravity dams in accordance with Fenves & Chopra [8]'s seminal work. In this chapter, first, the size of the model that is required to realistically simulate the wave propagation effects in a 2D domain is sought. Viscous dashpots are used in this model which can be later used in a time domain analysis including the nonlinear effects. The remaining part of the chapter focuses on the required changes in the damping ratio and the reduction to

the Young's Modulus of the foundation material of the USACE model. Such modifications are of value to practicing engineers as the aforementioned large domain model cannot be used in design offices. In such a way, the soil structure interaction effects can be "cheaply" added to the analysis without the added costs of modeling the domain.

3.2. Determination of the Model Size for Realistic Results

Results of the study conducted by Medina et al. [9], which can be treated as exact solutions, are compared to the results obtained in this study in the frequency domain to decide on the optimum model size which represents the response of the soil-structure system correctly. System used in the comparisons is presented in Figure 3.1, where H, B and H_f are height and base width of the dam and soil height, respectively. Below the soil layer on which the structure rests, a fixed boundary is assumed representing hard rock boundary. Relations between these parameters taken as $H_f/H=4$ and $B/H=0.8$, where the material properties are Young's Modulus= 27.5GPa, Poisson's ratio=0.20, unit weight=2.48t/m^3 (dam) and Young's Modulus= 27.5GPa, Poisson's ratio=0.33, unit weight=2.64t/m^3 (soil). A hysteretic 5% material damping is used for the whole system.
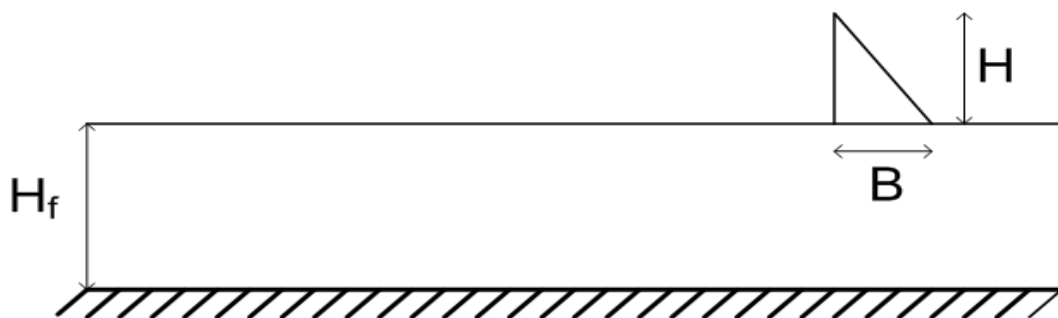

Figure 3.1. *BEM-FEM Comparison Model*

In the analyses solved with finite element method; 10B, 20B, 30B and 40B model widths are used, which is applied to both horizontal directions to determine model size. Viscous boundary elements are used at the side boundaries.

Comparison between the results of BEM and FEM solutions is given in Figure 3.2. As can be seen while 10B extended model gives inaccurate results in entire frequency range, 20B extended model shows the same inaccuracy in peak values. The other two models however, give reasonably accurate results as compared to BEM solutions except high frequency range where the difference is relatively insignificant. Since there is no significant difference between 30B and 40B extended models, 30B model size can be accepted as adequate. This domain size, as verified by comparison to exact solution, is used to represent the "correct" solution simulating the wave propagation effect in the media; analysis of the CFRD system on such a domain with 30B model size will be used in the following sections as the benchmark solution and referred in the proceeding comparisons as the "large" solution.

The reader of this study is kindly warned that success of this modeling approach is highly dependent on the aspect ratio of the elements constructed. As this ratio is distorted, the results tend to become unreliable, since complex eigen values start to occur [22].
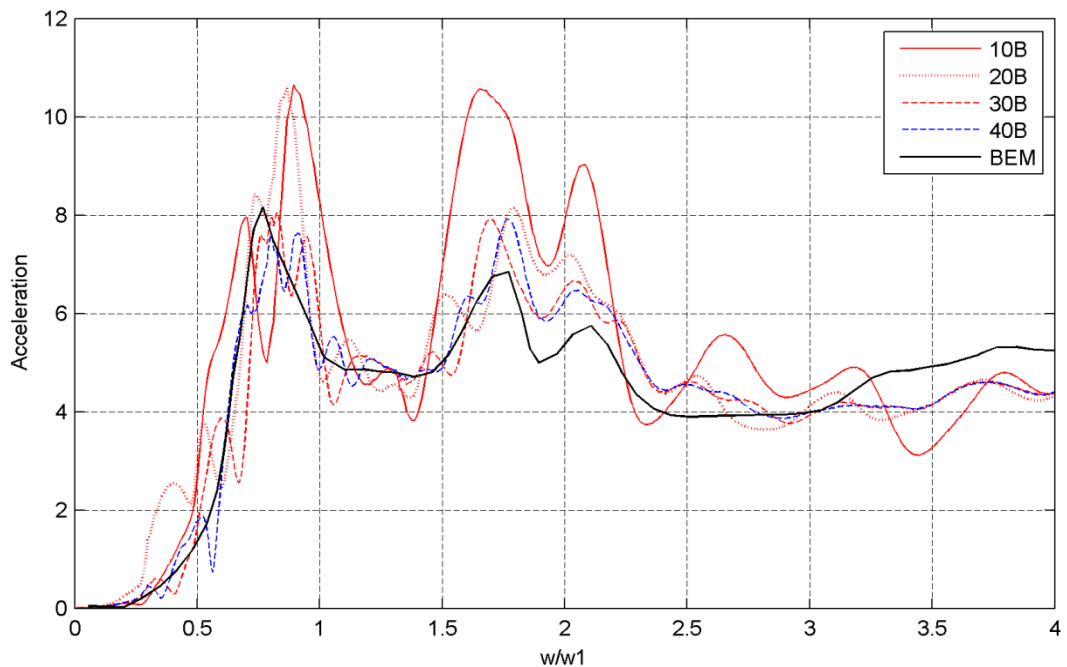

Figure 3.2. *Crest Acceleration Relative to Dam Base($H_f/H=4$)*

3.3. Equivalent Model, Modeling Details

As given above, the benchmark solution involves a significantly large FE model, which is too large to be employed in practical applications. Despite the fact that all computations provided above are linear, frequency based solutions, model sizes reached up to 140,000 degrees of freedom.

In current practice, the designers expect to simulate the behavior of a dam using manageable FE models, with low degree of freedom systems. Currently preferred approach is to model dams by considering only the superstructure or superstructure over a limited amount of soil by using plane strain models. If the layer below the dam is significantly more rigid than the structure, kinematic or inertial soil-structure interaction may be ignored, using a typical fixed base assumption. Otherwise, the typical approach [10] is to use a massless soil layer beneath the dam superstructure in accordance with the method proposed by Fenves & Chopra [8] (Figure 3.3). This model mainly shows a single peak response while somewhat considering period elongation. The model applies to dams on a semi-infinite soil layer, for dams resting on a layer of soil underlain by stiff rock, a provision is not currently provided. Accordingly, for the current study on which a CFRD is assumed to be built on layer of soil, the base boundary condition in the USACE model is changed from roller to the fixed support.
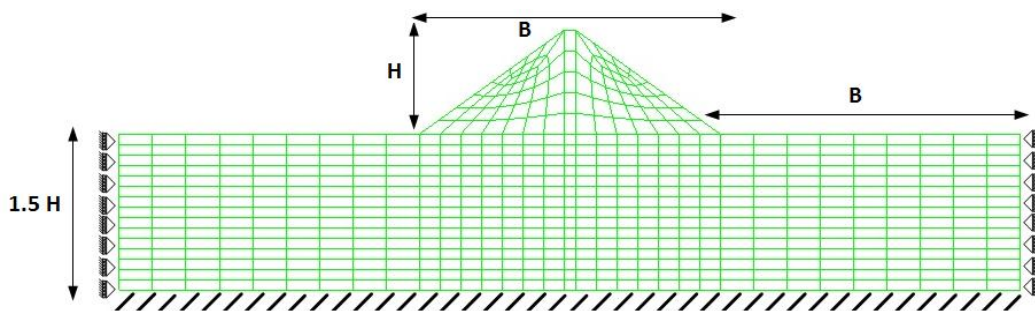

Figure 3.3. *Modified Equivalent USACE Model*

5% hysteretic damping for the soil layers is used in the benchmark solution in the following analyses. The damping in the modified USACE model is chosen to be

Rayleigh damping. The main reason to select the Rayleigh damping curve is its ability to make it possible to solve problems with nonlinear material models which is required for the analysis of CFRD dams. However, the use of Rayleigh damping induces significant increase in damping ratios at high frequencies and creates problems especially in comparison of acceleration quantities at high frequency range.

Two different software, i.e. DIANA and ANSYS [22][32]are used in the analyses. DIANA was used for the "large" solutions with large domains whereas ANSYS was utilized for the equivalent models. All mathematical models are formed by using 4-node plane strain elements (Figure 3.4) based on Gauss interpolation and 2-2 Gauss integration which yields constant axial strains in their defined direction and linearly varying in the other direction (3.1) [22][32]. Shear strain is constant over the entire element. From the element definition it can easily be seen that the used element can experience shear locking. In order to overcome this effect incompatible strain modes are applied by default by the used software [22][32]. In addition, element stiffness matrices are modified to show constant dilation over the element area [33].

$$u_i(\zeta,\eta) = b_0 + b_1\zeta + b_2\eta + b_3\zeta\eta \tag{3.1}$$

where;

b_0, b_1, b_2 & b_3 = Equation constants

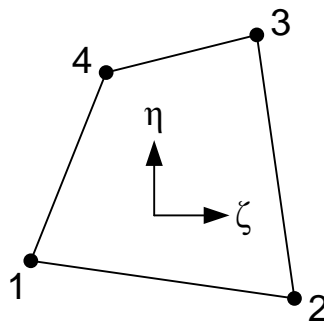ζ & η = Local Directions of integration

Figure 3.4. *4-Noded Plane strain Element*

3.4. Material and Geometrical Properties of the System Analyzed

Soil

Soil properties are mainly selected to represent three different soil types. These are rock (V_s=1000m/s, E_f=7040MPa), very dense soil and soft rock (V_s=500m/s, E_f=1760MPa) and stiff soil (V_s=300m/s, E_f=640MPa) respectively. Minimum value is selected as 300m/s in practice since shear wave velocities under this value is not common in dam construction sites [35]. Poisson's ratio and unit weight are assumed as 0.33 and 2.64t/m^3 respectively and kept constant in all analyses.

Dam

In this section, the dam superstructure is modeled linear elastic. Three different Young's Modulus values, representing a weak, medium stiff, and stiff rockfill material were represented choosing the moduli of the fill as 50, 150 and 300MPa. This range is selected in accordance with typical values provided in the literature [36]. The Poisson's ratio and the unit weight of the rockfill were assumed as 0.20 and 2.48t/m^3 respectively. Upstream and downstream slopes of the dam are assumed as 1.4 H to 1.0 V. Crest width and dam height are selected as 8m and 75m respectively. It should be noted that the geometrical properties of the dam are selected analogous to Cokal Dam (Figure 3.5) built in the Thracian region of Turkey (except for the thalweg geometry). The first three fundamental frequencies of the models formed with these properties are 0.418, 0.714 and 1.02Hz respectively (Figure 3.6).

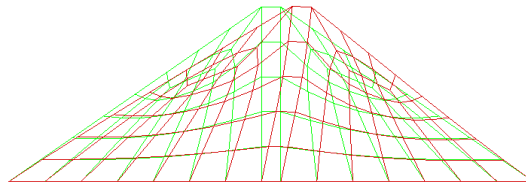**Figure 3.5.** *Cokal Dam in Construction*

Figure 3.6. *Fixed Base First Fundamental Mode Shape(0.418, 0.714 & 1.02Hz for E=50, 150 and 300MPa, respectively)*

3.5. The Basis of Comparison

Comparisons are made by limiting the frequency of interest at 10Hz and solving the systems at 200 different frequency values. The main objective is to compare the responses both in amplitude and the occurrence frequency. Unit ground acceleration is applied to the system at all frequencies at the base of the models. Modified USACE results are named as "approximated" results while the 30B extended model results are provided now on as the "large" results (Table 3.1). Rayleigh damping parameters a_0 & a_1 are changed so as to determine the best approximate model response that fits closely to the "large" result.

The best Rayleigh parameters for a particular combination of dam and foundation stiffness are determined by minimizing the error between the displacement responses of both models using mean squared error $MSE(\hat{\lambda}) = E[(\hat{\lambda} - \hbar)^2]$ along the frequency range in interest, where $\hat{\lambda}$ & $\hbar$ are the large and approximate results, respectively.

A very important issue met during the analyses was the inability of the USACE model to predict the fundamental mode of a CFRD foundation composite system when compared to 30B extended models. Inclusion of damping does not change the fundamental frequency observed for the system, but modifies the amplitude of the transfer function. For this reason, especially in soft dam and stiff foundation combinations, another parameter was added to predict the first natural frequency of the system correct. Young's Modulus of the foundation layer was changed (reduced) by multiplying the original foundation modulus with a factor denoted as 'δ' so as to

obtain the fundamental frequency of the approximate model in sync with the "large" solution.

Frequency range was limited in the calculations as the fundamental frequencies of CFRDs are significantly small due to the low modulus of the fill. The error quantity that was minimized was therefore calculated from 0Hz to 3 times the fundamental mode of the system. It should be noted that the fundamental mode mentioned is the elongated composite system frequency.

Table 3.1. *Model Comparison Table*

Model	Function	Explanation
Large	Used for the simulation of correct solution of dam resting on layered media.	30B extended to both sides, fixed at the, base viscous boundary at the sides.
USACE (Approx.)	Used from a practical engineering point of view, fast analysis.	B extended to the sides, 1.5H depth, pinned at the boundaries.
Fixed		Fixed at the base of the dam body, no foundation is modeled.

3.6. Modeling Assumptions

All simulations made by mathematical models contain several assumptions which can differ depending on the actual behavior of the simulated geometries in real life. In addition, since two different programs are used to make the comparison possible, differences due to the software used must also be minimized. In this respect, the assumptions made in the analyses are listed as follows:

- Rockfill dams with large crest width/depth aspect ratios are usually modeled in accordance with plane strain modeling concepts. The model used for the CFRD dam in this study is also a plane strain model.
- The main objective of this chapter is to assess the performance of the equivalent models both in amplitude and occurrence frequency. In order to

focus on the objective of investigation of the importance of SSI on these factors, the behavior of the system was assumed to be linear. Nonlinearity in rockfill properties and the concrete face slab is going to be incorporated in the models in the next section.

- Hydrodynamic effects are ignored by not modeling the impounding water mass. Dam-reservoir interaction was observed to be significant in concrete dams on hard rock (response in high frequency range), but its importance was mentioned to diminish as the relative importance of soil flexibility increases (as in the case of CFRDs).

- Since the slab geometry can be semi-independent from the properties of the dam body and cannot be estimated exactly without a proper design procedure, modeling of the face slab is not included in the simulation.

- Main reason to use 4-noded plane strain elements is their low degree of freedom number that reduces size of the solution matrices. As mentioned earlier these elements have constant shear strain over its area. Even though this is not the case in reality, since the mesh density used is fine enough to simulate the behavior there is no inadequacy observed in simulations.

- Constant dilation is assumed over the element area to make all stiffness matrix calculations identical in both programs.

3.7. Analysis Results and Discussions

The comparison of the displacement and acceleration responses of the "large" and "approximate" solutions, using the extended domain model and the USACE model, respectively, are provided below. The response quantities obtained are determined relative to dam base under unit ground acceleration at each frequency. Three different layer depths were utilized in the analyses, i.e. 1, 2 and 4 times the dam height, respectively. Maximum model depth is limited to 4H since this assumption yields a close enough approximation to half-space idealization and the difference when compared to the 8H model depth was insignificant. The comparison between the 4 and 8H models, along with the solutions from Fenves & Chopra [8] and Medina et al. [9] for a semi-infinite base under the dam is provided in Figure 3.7.

As mentioned before, modified USACE model results and 30B extended model results are denoted as "approximated" and "large" results respectively. Rayleigh parameters and the corresponding damping ratio for the elongated fundamental modes are also presented below for the results obtained from different dam-foundation stiffness combinations (i.e. V_s=300, 500, 1000m/s) and different foundation depth combinations (H, 2H, 4H). Comparisons are given in limited frequency range by considering each case independently, since the displacement response tends to get smaller and insignificant in higher frequencies. For acceleration comparisons, results are presented along the whole computation range. Frequency values located in the x-axis, are normalized by the fixed base first fundamental frequencies (w_1) of the corresponding dams.
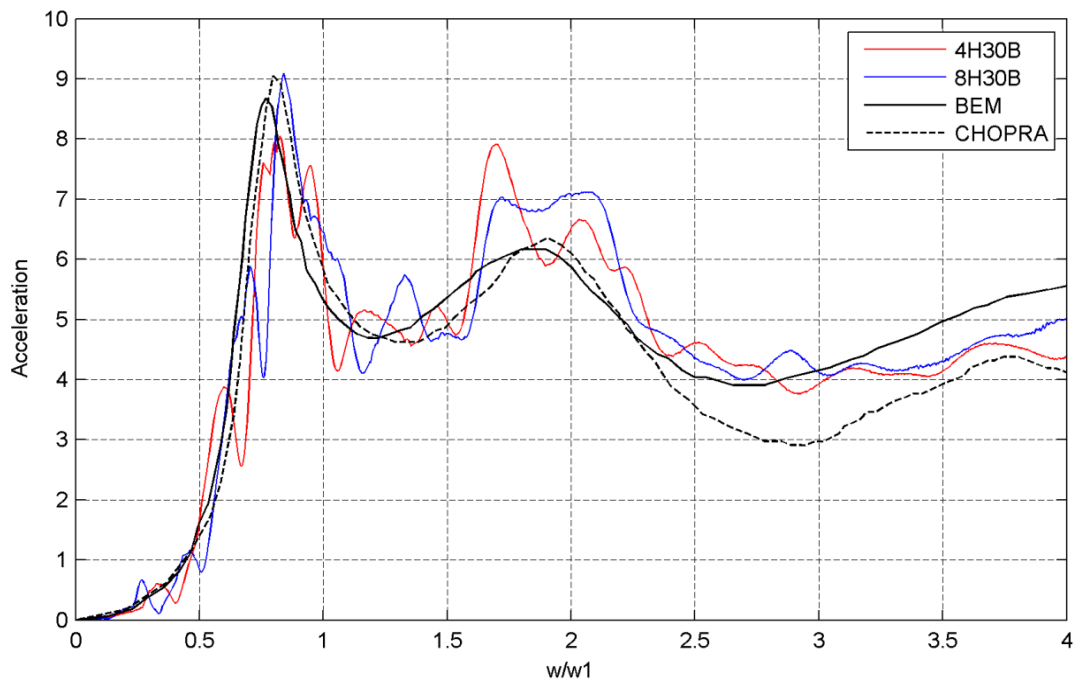

Figure 3.7. *Crest Displacement Relative to Dam Base(Half Space Idealization)*

3.7.1. The Case where Young's Modulus of the Dam is 50MPa

Crest Displacement

When the Young's Modulus of the dam was assumed as 50MPa, relative displacements observed at the dam crest are simulated substantially accurate with modified USACE model (Figure 3.8, Figure 3.9 and Figure 3.10). Fixed base model

results start to become inconsistent as expected as the shear wave velocity of the soil decreases. Obtained peak results are almost at the same frequency in all models, regardless of the foundation stiffness, and they tend to decrease as the shear wave velocity of the soil decreases. For this case, the minimum V_s assumed points out to as much as 10 times the stiffness of the dam for the foundation; within the range of the stiffness assumed for foundation, foundation modeling is not necessary to determine the fundamental frequency of the joint system correct. However, it is clearly seen that the depth of the foundation significantly changes the amplitude of the maximum response. For a deep foundation, a much lower peak response at the crest was obtained, when compared to the results from the models with shallow foundations underlying the dam.

Crest Acceleration

As can be seen in Figure 3.11, Figure 3.12 and Figure 3.13, relative accelerations observed at the dam crest are successfully simulated with modified USACE model at low frequencies. Inconsistency of the results at the high frequencies can be explained with the increase in damping ratio because of Rayleigh damping. As a proof to this observation, the fixed base model yields more accurate results at high frequencies when compared to modified USACE model. Similar to the trend above, the simulations conducted with fixed base model starts to become inconsistent depending on the shear wave velocity of the soil like the displacement response.

Rayleigh Damping Curve Parameters

Rayleigh damping parameters used in displacement and acceleration comparisons that reduce the error calculated along the frequency range in interest to minimum. When the graph (Figure 3.14) showing the damping ratios is observed, it can be seen that equivalent damping ratios tend to increase in parallel to the decrease in shear wave velocity of the soil and these ratios are directly proportional to depth of the soil layer. For the dam underlain by a deep deposit with V_s=300m/s, (that is almost 10 times stiffer than the dam body), it is observed that simplified modeling should incorporate an additional 5% damping to simulate the radiation effect properly.
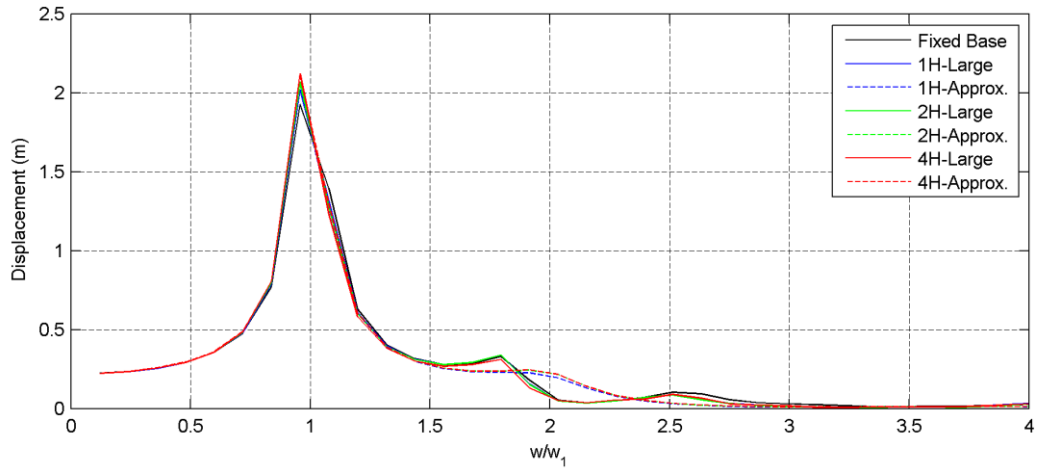
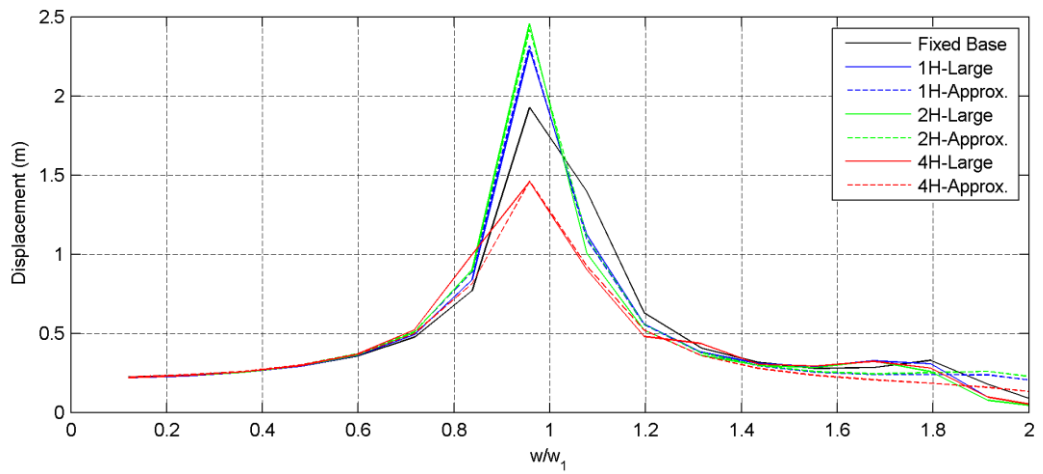**Figure 3.8.** *Crest Displacement Relative to Dam Base(E=50MPa,V_s=1000m/s)*

Figure 3.9. *Crest Displacement Relative to Dam Base(E=50MPa,V_s=500m/s)*

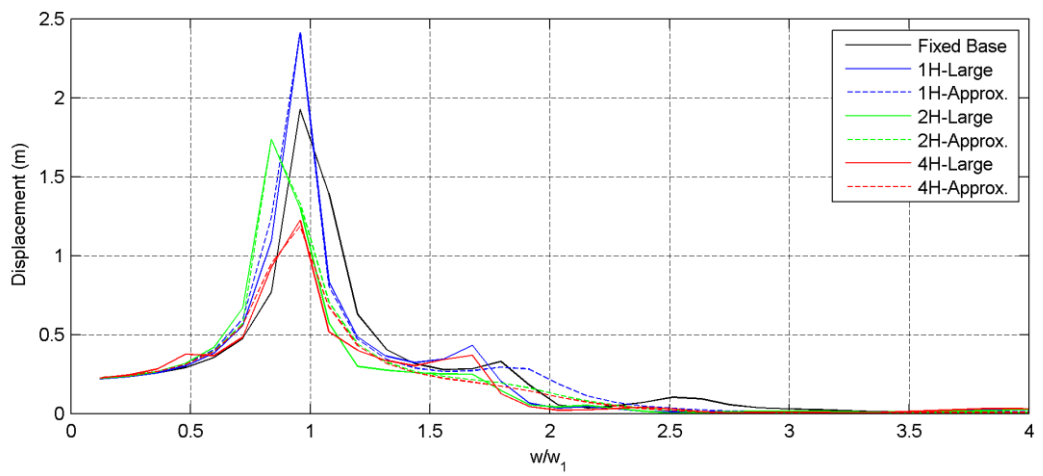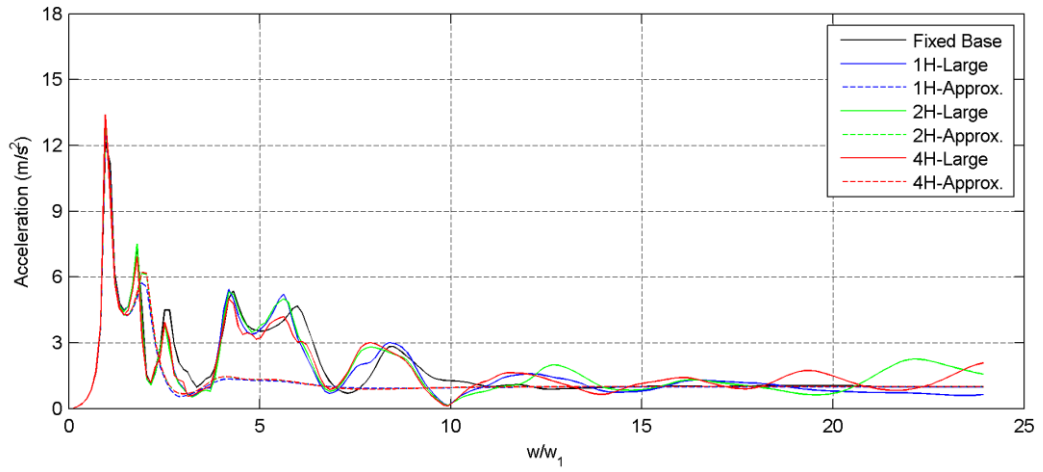**Figure 3.10.** *Crest Displacement Relative to Dam Base(E=50MPa,V_s=300m/s)*

Figure 3.11. *Crest Acceleration Relative to Dam Base(E=50MPa,V_s=1000m/s)*

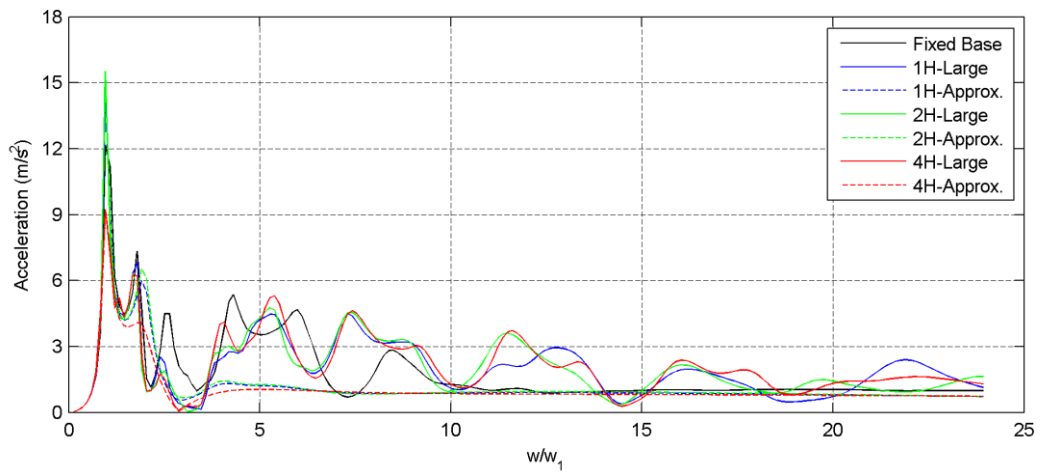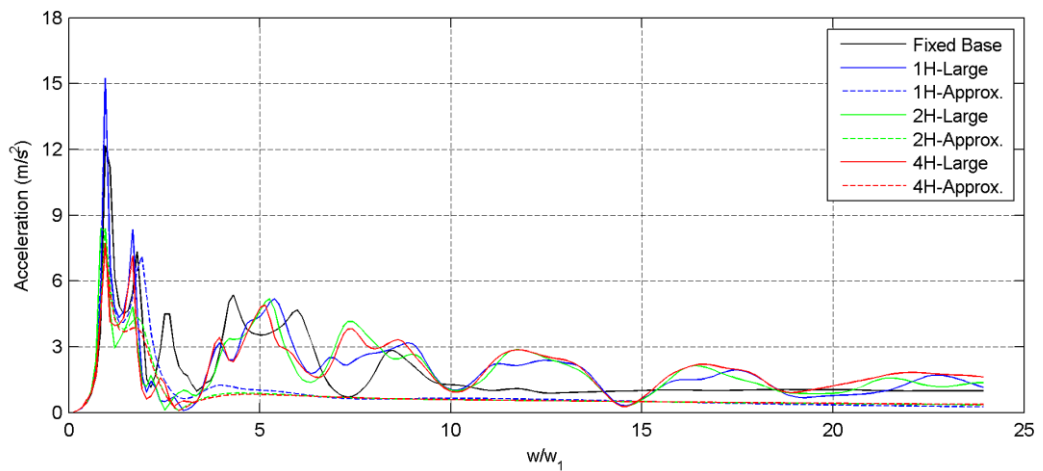**Figure 3.12.** *Crest Acceleration Relative to Dam Base(E=50MPa,V_s=500m/s)*

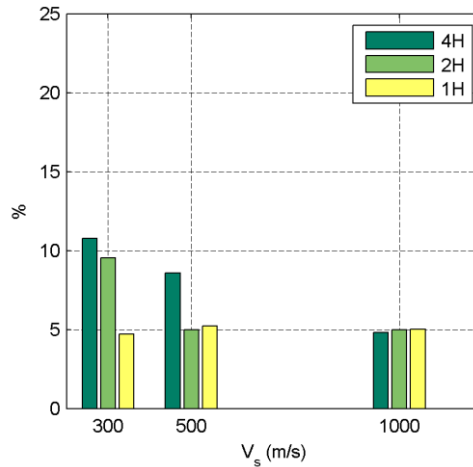**Figure 3.13.** *Crest Acceleration Relative to Dam Base(E=50MPa,V_s=300m/s)*

Figure 3.14. *Variation in Damping Ratio Applied to First Peak Frequency with respect to Layer Depth and Shear Wave Velocity(E=50MPa)*

Another matter that should be considered is that damping ratios calculated for 1H soil depth are somewhat below 5% at low shear wave velocities and reach equilibrium at 5% as the soil becomes stiffer. This unexpected and yet numerically insignificant behavior is considered to be the result of the numerical error during calculations. Similar to this fact, damping ratio reduces as the soil becomes stiffer and reaches a value somewhat lower than 5% in 4H model.

3.7.2. The Case where Young's Modulus of the Dam is 150MPa

Crest Displacement

When the Young's Modulus of the dam was assumed as a moderate value of 150MPa, relative displacements observed at the dam crest are simulated substantially accurate with modified USACE model (Figure 3.15, Figure 3.16 and Figure 3.17) for sites having high shear wave velocities. Second peaks start to emerge in the response as the shear wave velocity of the soil reduces, but since these peaks have relatively lower values, approximation by the simplified model can still be considered as accurate to some extent. For this case, the results from the fixed base model start to differ at peak values both in value and the occurrence frequency as the shear wave velocity of the soil decreases. Period elongation becomes an issue; depending on the layer depth a reduction in the model properties of the foundation in the simplified model had to be employed; δ factor is taken as

0.67 and 0.33 for 500 and 300m/s soil shear wave velocities respectively, for the 2H and 4H models.

Crest Acceleration

As can be seen in Figure 3.18, Figure 3.19 and Figure 3.20, relative accelerations observed at the dam crest are successfully simulated with the modified USACE model at low frequencies. Inconsistency of the results at high frequencies can be explained with the increase in the damping ratio because of the utilization of Rayleigh damping as in the previous case. As expected, fixed base model yields more accurate results as compared to modified USACE model at high frequencies. But in addition to the cons of fixed base model in previous case, occurrence frequencies of the peak responses start to differ.

Rayleigh Damping Curve Parameters

Rayleigh damping parameters used in displacement and acceleration comparisons that reduce the error calculated along the frequency range in interest to minimum. If the graph (Figure 3.21) showing the damping ratios is observed, it can be seen that equivalent damping ratios tend to increase in parallel to the decrease in shear wave velocity of the soil and these ratios are directly proportional to depth of the soil layer, as in previous case. The significance of the results for the dam underlain by the weakest soil layer should be mentioned. If the dam is underlain by a deep soil deposit, as high as 20% damping (additional 15%) should be used in the analyses in the simplified model. If the dam is underlain by a stiff soil layer approximately equal to the height, no additional damping was determined to be necessary in the simulations. Hence, for the stiffness ratio of $E_f/E_d=4$, the damping utilized for the simplified USACE model is largely dependent on the layer depth. However what is notable is that for a 1H layer depth, the amplitude of the peak response is larger than the fixed base result which signifies the trapping of the waves in such a layer. The modeling of this response with a fixed base model for $E_f/E_d<4$ does not seem conservative.

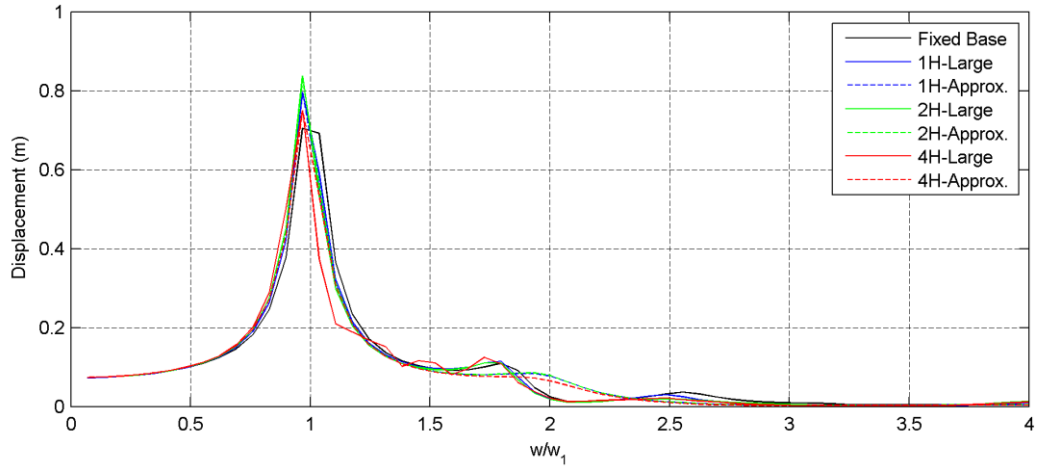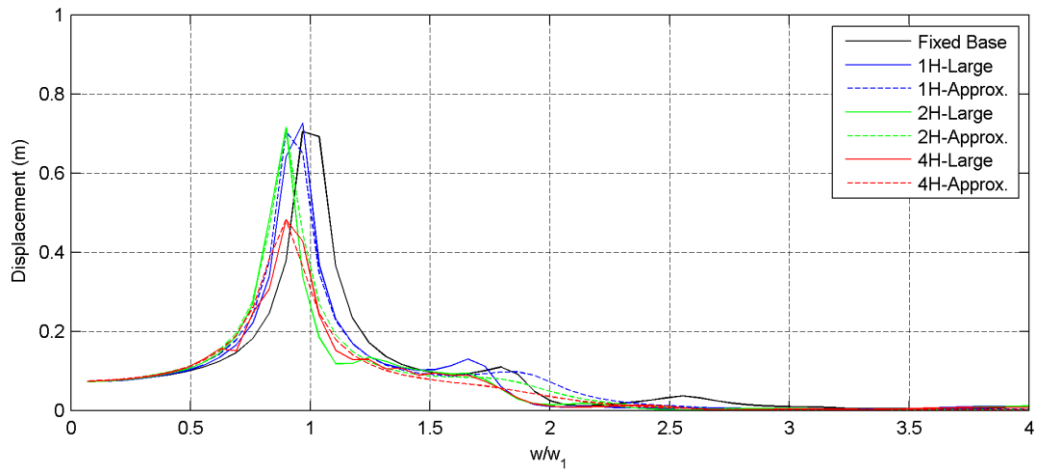**Figure 3.15.** *Crest Displacement Relative to Dam Base($E=150MPa, V_s=1000m/s$)*

Figure 3.16. *Crest Displacement Relative to Dam Base($E=150MPa, V_s=500m/s$)*

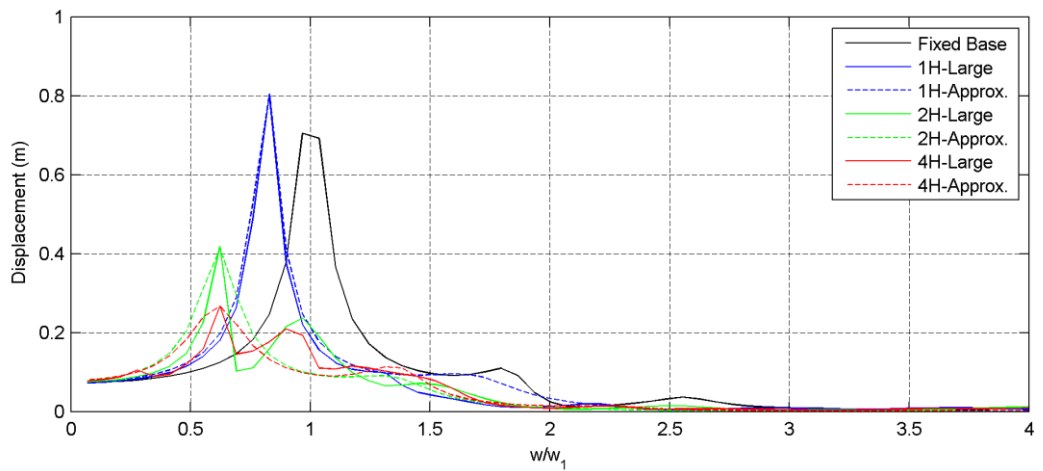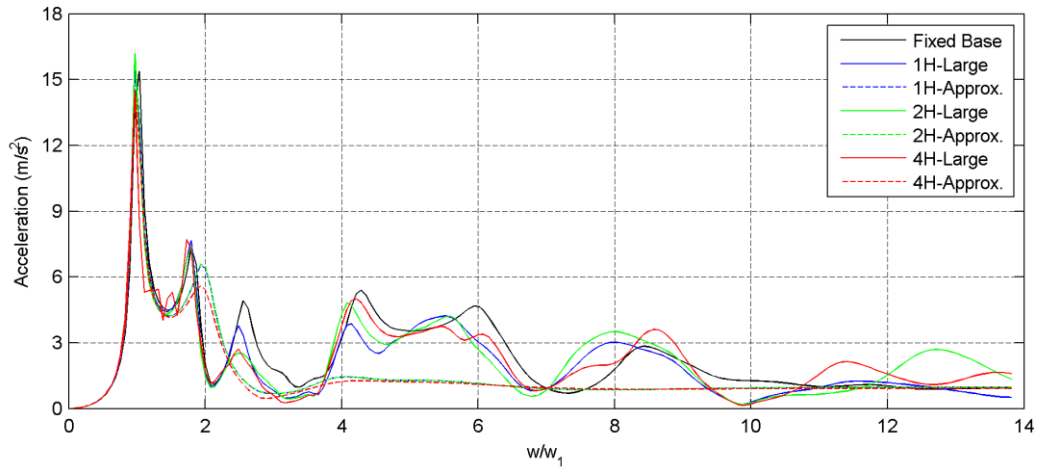**Figure 3.17.** *Crest Displacement Relative to Dam Base($E=150MPa, V_s=300m/s$)*

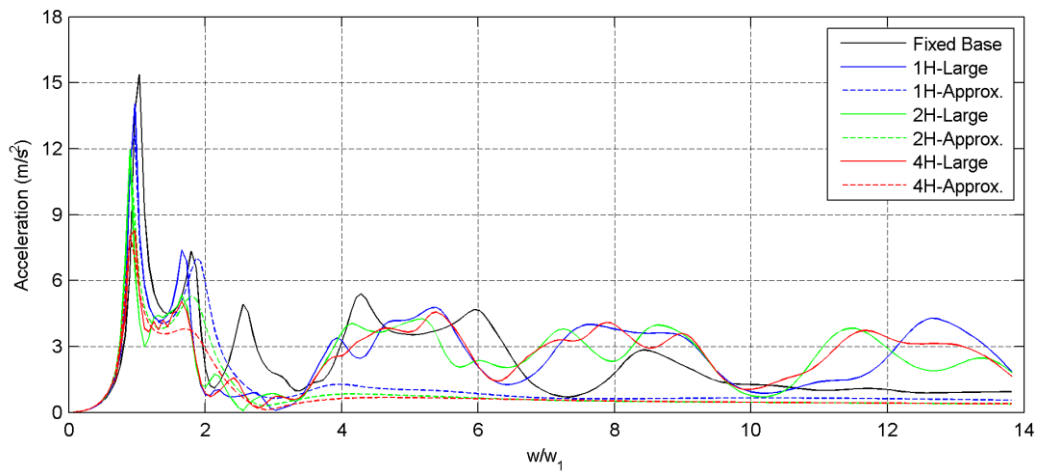**Figure 3.18.** *Crest Acceleration Relative to Dam Base(E=150MPa,V_s=1000m/s)*

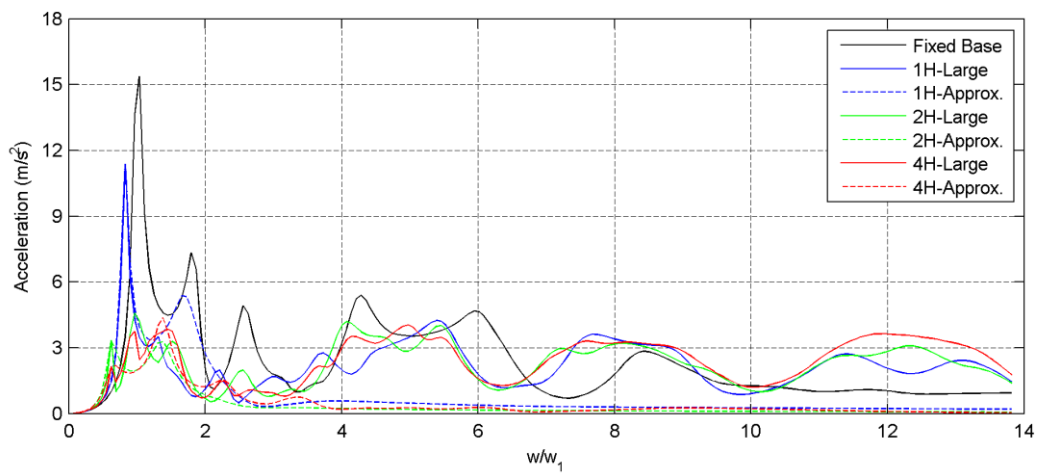**Figure 3.19.** *Crest Acceleration Relative to Dam Base(E=150MPa,V_s=500m/s)*

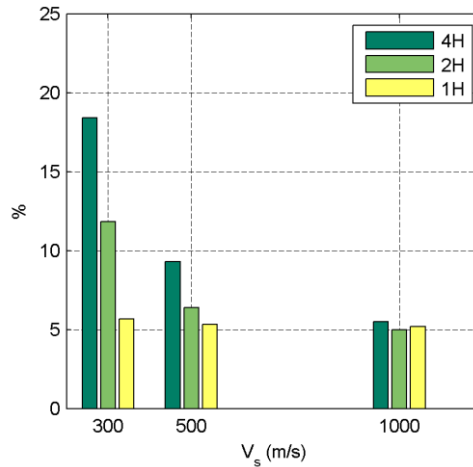**Figure 3.20.** *Crest Acceleration Relative to Dam Base(E=150MPa,V_s=300m/s)*

41

Figure 3.21. *Variation in Damping Ratio Applied to First Peak Frequency with respect to Layer Depth and Shear Wave Velocity(E=150MPa)*

3.7.3. The Case where Young's Modulus of the Dam is 300MPa

Crest Displacement

When the Young's Modulus of the dam has a high value 300MPa which can only be observed in well-compacted gravel dams, relative displacements observed at the dam crest are simulated substantially accurate with modified USACE model (Figure 3.22, Figure 3.23 and Figure 3.24) only at very stiff rock sites. Second and even third peaks start to emerge in the frequency response as the shear wave velocity of the soil reduces. Especially for the soft sites, use of the modified USACE model results in an insufficient performance for simulation of the response. On the other hand, the fixed base model is not adequate as well; it yields completely different responses at peak values both in value and the occurrence frequency as the shear wave velocity of the soil decreases and creates an entirely different behavior. As in previous case period elongation increases depending on the depth increase and to catch this elongation δ factor is taken as 0.40 and 0.26 for 500 and 300m/s soil shear wave velocities respectively, both at 2H and 4H models.

The figures for the displacement response function also show that as the stiffness of the dam and the foundation approach it each other, additional response peaks are observed in the frequency response. However, this phenomenon is also dependent

42

on the layer depth; only for the underlain by deeper stratums these peaks are observed.

Crest Acceleration

As can be seen in Figure 3.25, Figure 3.26 and Figure 3.27, relative accelerations observed at the dam crest are correctly simulated with modified USACE model only at low frequencies and first peaks. But as the frequency gets higher, models start to give inconsistent results both in the value and the occurrence frequency. As expected, the fixed base model gives more accurate results as compared to modified USACE model at high frequencies. But it shows completely unrealistic behavior almost along the whole frequency range, especially at low frequencies.

Rayleigh Damping Curve Parameters

Rayleigh damping parameters used in the displacement and acceleration comparisons that reduce the error calculated along the frequency range in interest to a minimum. If the graph (Figure 3.28) showing the equivalent damping ratio at the first mode is observed, the downward trend of the damping ratio with increasing soil stiffness can be observed to be more significant compared to previous cases. Moreover, the radiation effects were observed to be more pronounced. For a dam-foundation system with similar stiffness values, if the foundation layer is substantially deep, as high as 20% damping should be utilized in the simpler models to simulate the radiation damping. The additional damping to be employed reduces very quickly depending on the layer depth. For a 1H deep soil stratum underlying the dam, very small additional damping is observed to be needed.

Another important point to be noticed is that while very high additional damping is prescribed for simple model of a CFRD underlain by a 4H deep layer, the general picture of the response spectrum indeed shows that such a model would have a very hard time in representing the higher peaks in the response that is observed as the foundation layer gets deeper. However, for shallow foundations, the simpler model performs much better in approaching the "exact" solution with domain modeling.
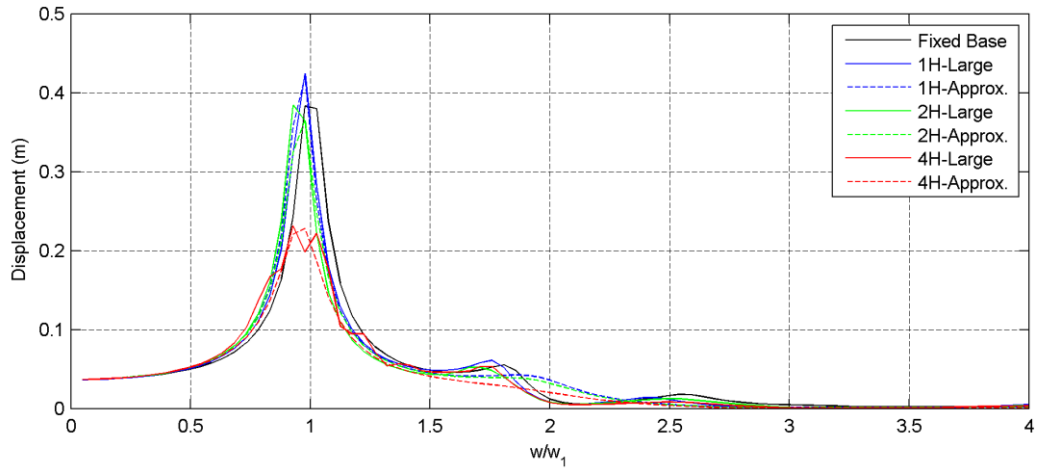
Figure 3.22. *Crest Displacement Relative to Dam Base(E=300MPa,V_s=1000m/s)*
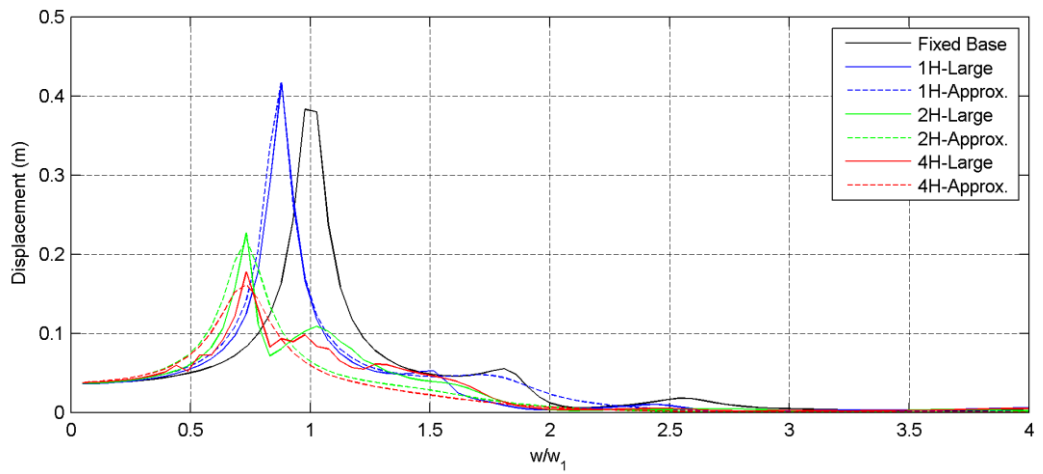
Figure 3.23. *Crest Displacement Relative to Dam Base(E=300MPa,V_s=500m/s)*

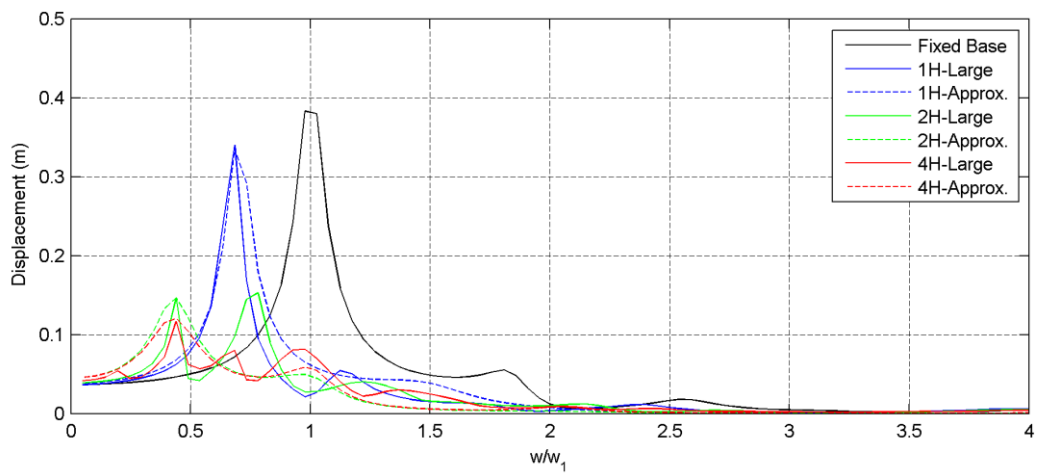**Figure 3.24.** *Crest Displacement Relative to Dam Base(E=300MPa,V_s=300m/s)*
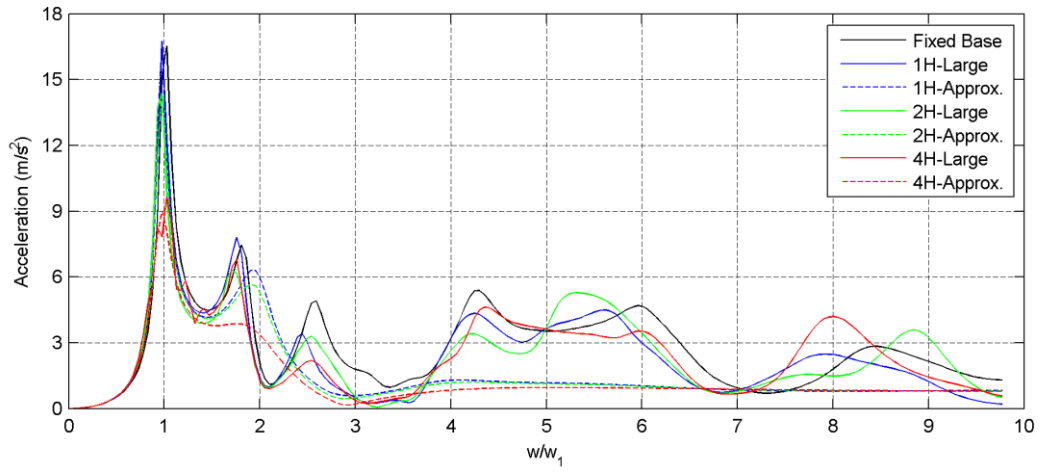
Figure 3.25. *Crest Acceleration Relative to Dam Base(E=300MPa,V_s=1000m/s)*
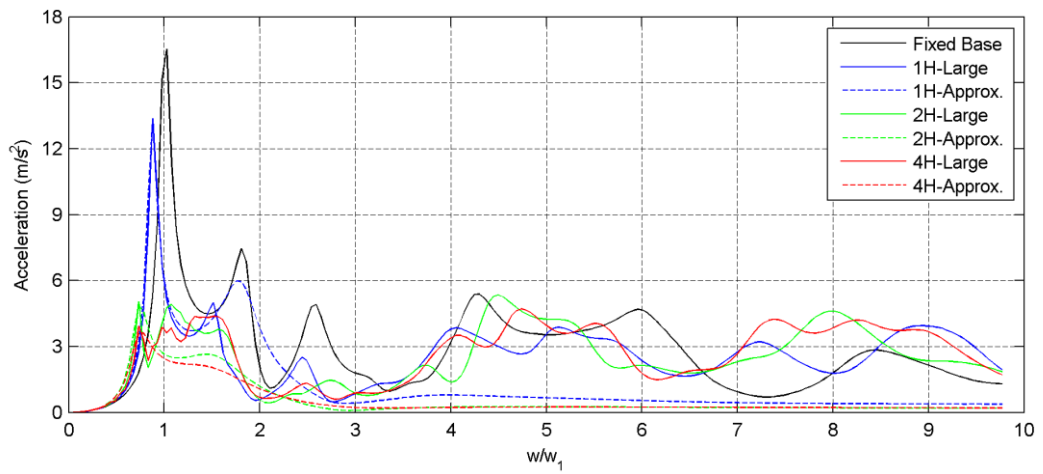
Figure 3.26. *Crest Acceleration Relative to Dam Base(E=300MPa,V_s=500m/s)*
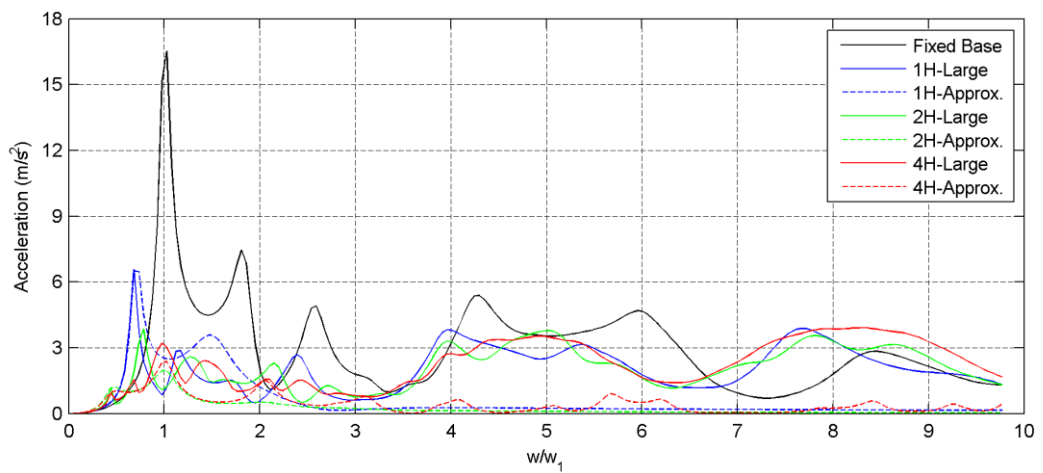
Figure 3.27. *Crest Acceleration Relative to Dam Base(E=300MPa,V_s=300m/s)*
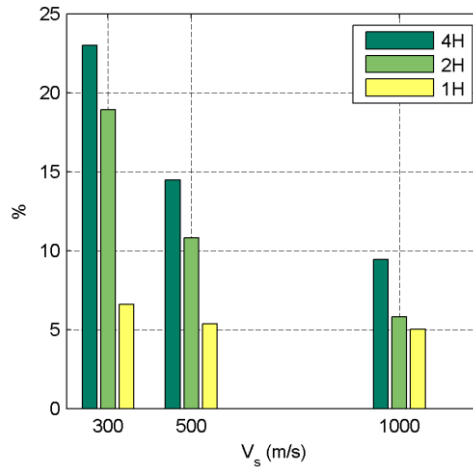
Figure 3.28. *Variation in Damping Ratio Applied to First Peak Frequency with respect to Layer Depth and Shear Wave Velocity(E=300MPa)*

3.7.2. Equivalent Damping Ratio and Displacement Response in General

Although it is partially discussed previously in each case how the equivalent damping ratios change depending on the soil depth change, it is useful to make a general commentary by looking at the overall situation. It can be said that equivalent damping ratios for the simplified model increases as the moduli of the dam approaches to the soil and /or as the soil deposit deepens (Figure 3.29). This finding implies that, for example, the analysis of a stiff gravel fill dam (E~300MPa) over an alluvium layer (E~500-600MPa) is not a straightforward task of assuming 5% of damping and conducting analyses. The depth of the layer behind the dam significantly increases the damping of the first mode, and changes the frequencies of the system. One would significantly underestimate the damping using a simplified analysis procedure in this case.
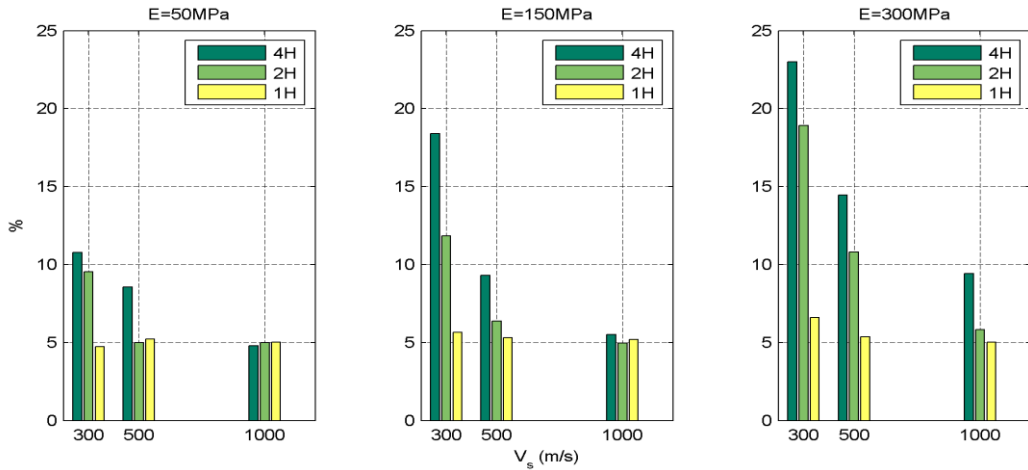
Figure 3.29. *Variation in Damping Ratio Applied to First Peak Frequency with respect to Layer Depth and Shear Wave Velocity for 3 Different Dam Moduli*

A similar comment can also be drawn based on the displacement responses given in the previous figures. The results from the models with 30x model width imply that (as summarized in Figure 3.30), the displacement demand on the dam, relative to its base increases as the soil deposit gets more shallow. As expected, this demand also increases as the moduli of the dam gets softer. Also except for the model in which the dam was assumed to have a low modulus of 50MPa, it can be concluded that natural vibration modes of the systems increases as the soil deepens. It should be noted that these displacement responses are belong to the large models, thus represent the "large" solution.
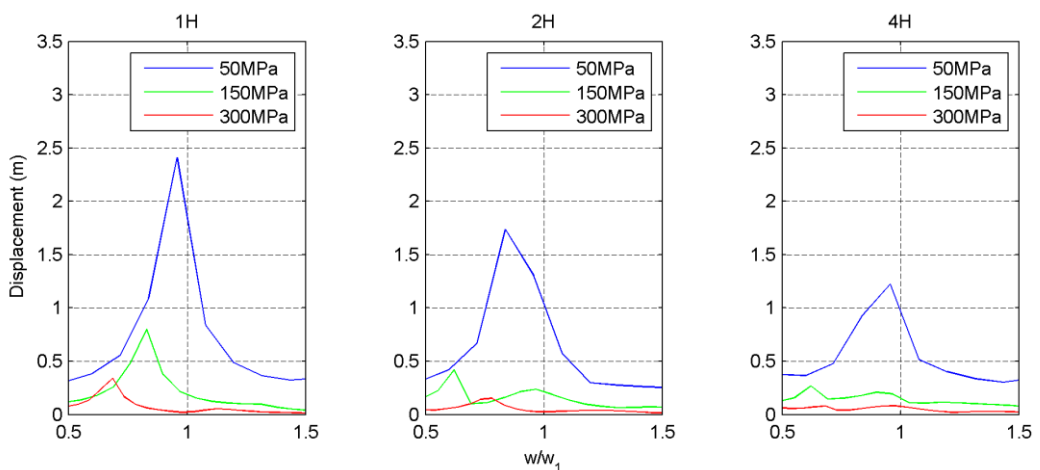
Figure 3.30. *Crest Displacement Relative to Dam Base for 3 Different Soil Depths (V_s=300m/s)*

CHAPTER 4

NONLINEAR RESPONSE OF CFRDS USING SOIL STRUCTURE INTERACTION

4.1. Introduction

In this chapter of the study, CFRD nonlinear response is investigated for different soil depths while considering the effect of soil structure interaction. Only 30B extended models are used to simulate the behavior and the changes in the responses corresponding to depth change are investigated.

4.2. Simulated Dam and Site Conditions of Interest

As given in the previous chapter, the dam of interest is the Cokal Dam located in the north-west Turkey in the Thracian peninsula which is less than 10km away from the extension of North Anatolian Fault system, which is constructed for irrigation and flood prevention purposes.

Soil beneath the dam superstructure is taken as a stiff soil corresponding the NEHRP, i.e. V_s=300m/s, which is not identical to the original site conditions. This alteration is made to observe the foundation effects more significantly. On the contrary, there is no alteration made to the original material or geometrical properties of the superstructure unlike the previous chapter. Since the constitutive

material properties are described previously in Chapter 2, only geometrical features are explained in this chapter.

4.3. Geometrical Features

Geometrical features of the whole system in interest are explained in detail in the following paragraphs. All alterations to the original geometrical features are also noted.

4.3.1. Superstructure

The geometry of the Cokal Dam is given in detail in Figure 4.1. The dam height is 83m from thalweg to the crest with a crest length of 605m. The base-width of the dam is 229.2m, measured from the top view. It should be noted that in practice thalweg part is embedded into the soil after a proper excavation, so this feature is taken into consideration while the model is constructed. The face slab thickness was taken as 50cm with a 0.3% reinforcement ratio as in the original design.

4.3.2. Soil

Soil beneath the dam superstructure is modeled analogous to the previous chapter. A stiff soil (V_s=300m/s) is assigned to the soil in the simulations. The effect of different soil depths 1H, 2H, 4H are taken into consideration.

(a) Cokal Dam Preliminary Design

(b) Cokal Dam Finite Element Model

(c) Finite Element Model Detail
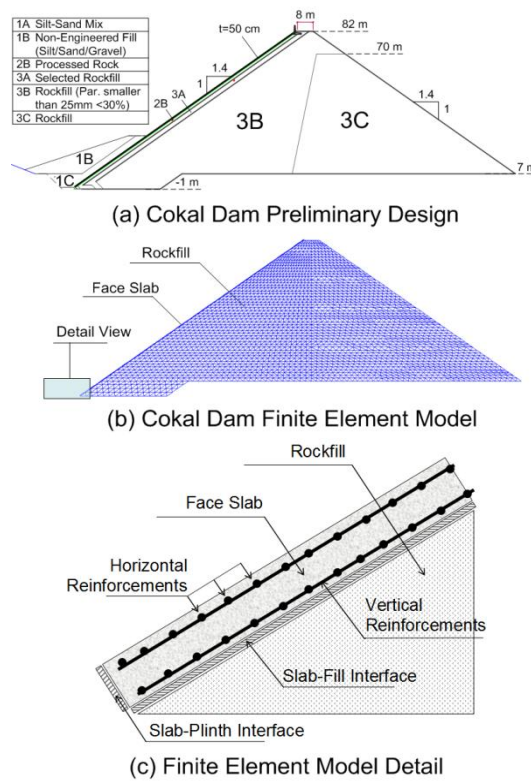
Figure 4.1. *Cokal Dam Geometrical Features [21]*

4.4. Computational Procedure and Analysis Methodology

Dam body, soil and viscous boundaries are formed by using same elements as explained in detail in previous chapters. Face slab, plint and interfaces are assumed to be constructed after the proper placement of the fill. Thus, a maximum number of 260,000 degrees of freedom system is created in a model depth of 4-H.

Face slab is formed by using 3-noded infinite shell elements based on 3x7 simpson integration with the following element formulation, which yields linearly varying axial strains(4.1) [22]. Although defining 3-point integration makes the element sensitive for shear locking, no such behavior is observed in the analysis.

$$u_i(\zeta) = a_0 + a_1\zeta + a_2\zeta^2 + (b_0 + b_1\zeta + b_2\zeta^2)\eta \qquad (4.1)$$

where;

a_0, a_1, a_2, b_0, b_1 & b_2 =Equation constants

ζ & η =Local Directions of integration

The interface between the slab and the fill is formed by using 6-noded interface elements between two lines based on quadratic elimination and 5 point Newton-Cotes integration [22]. The plint is formed by using 2-noded point interface element at the base of the slab which basically acts as a spring system.

Impounding of water is modeled as hydrostatic pressure acting on the face slab and considered to be completed in 27 stages. Hydrodynamic effect of water in the reservoir is not considered in the analysis. Thus, reservoir-soil and reservoir-structure interaction is out of scope.

After the impounding, ground motion is applied as "within" motion acting at the base of the mathematical model. The utilized ground motion is an Operation Based Earthquake (OBE) generated after a detailed seismic risk analysis for the actual dam site. A general appearance of the model can be seen in Figure 4.2.
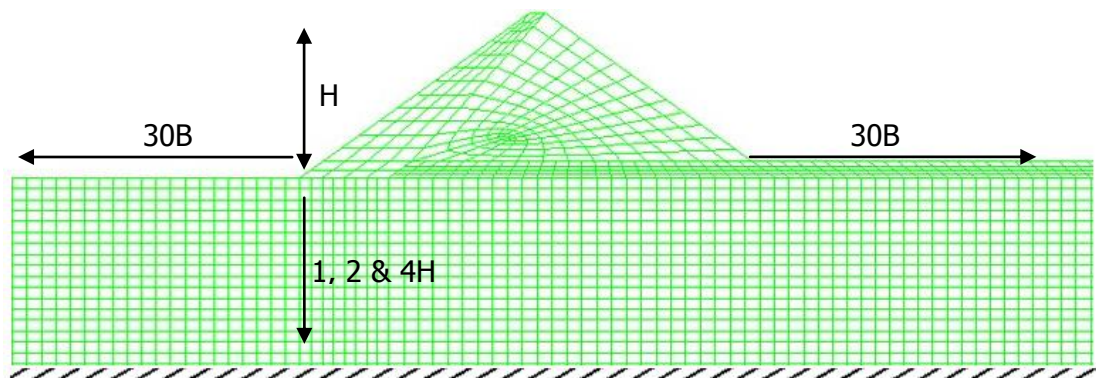
Figure 4.2. *Mathematical Model used in Nonlinear Analysis*

Crack widths on the face plate are computed using an empirical equation(4.2) [37], which is also commonly used in reinforced concrete design [38].

$$w_{\max} = 2.2\beta_{sg}\varepsilon_{scr}\sqrt[3]{d_c A_c}$$ (4.2)

where;

$w_{\max}$ =Maximum crack width

β_{sg} =Coefficient accounting for strain gradient

ε_{scr} =Strain in reinforcing bar at crack location

51

d_c =Distance from the extreme tension member to the center of the closest bar

A_c =Effective area of the concrete surrounding each bar

Results presented in the related figures are the averaged crack widths per unit length of the face slab, i.e. they signify the summation of crackwidths on the slab within the plane of the slab in a given meter.

4.5. Analyses Results and Discussions

In all 3 mathematical models the most important parameters to check are considered to be;

- Accelerations; to be able to observe the amplifications on the model.
- Crest displacements; since they give a general idea about to structural response.
- Axial stresses occurring on the face slab; to be able to observe the performance of the face slab.
- Crack openings on the face slabs; to see if there will be a possible leakage problem.

4.5.1. Accelerations

Ground motions applied to the models and their response on surface of the soil at 15H away from the downstream of the dam (denoted as mid-domain in the graphs) are given in Figure 4.3. It should be noted that all applied ground motions are generated from the same outcrop rock motion data and applied as within motions at the base of the models. As expected there is no trend in responses depending on the depth change. But it can be said that all mid-domain responses are amplified containing more strong peaks both in magnitude and amount.
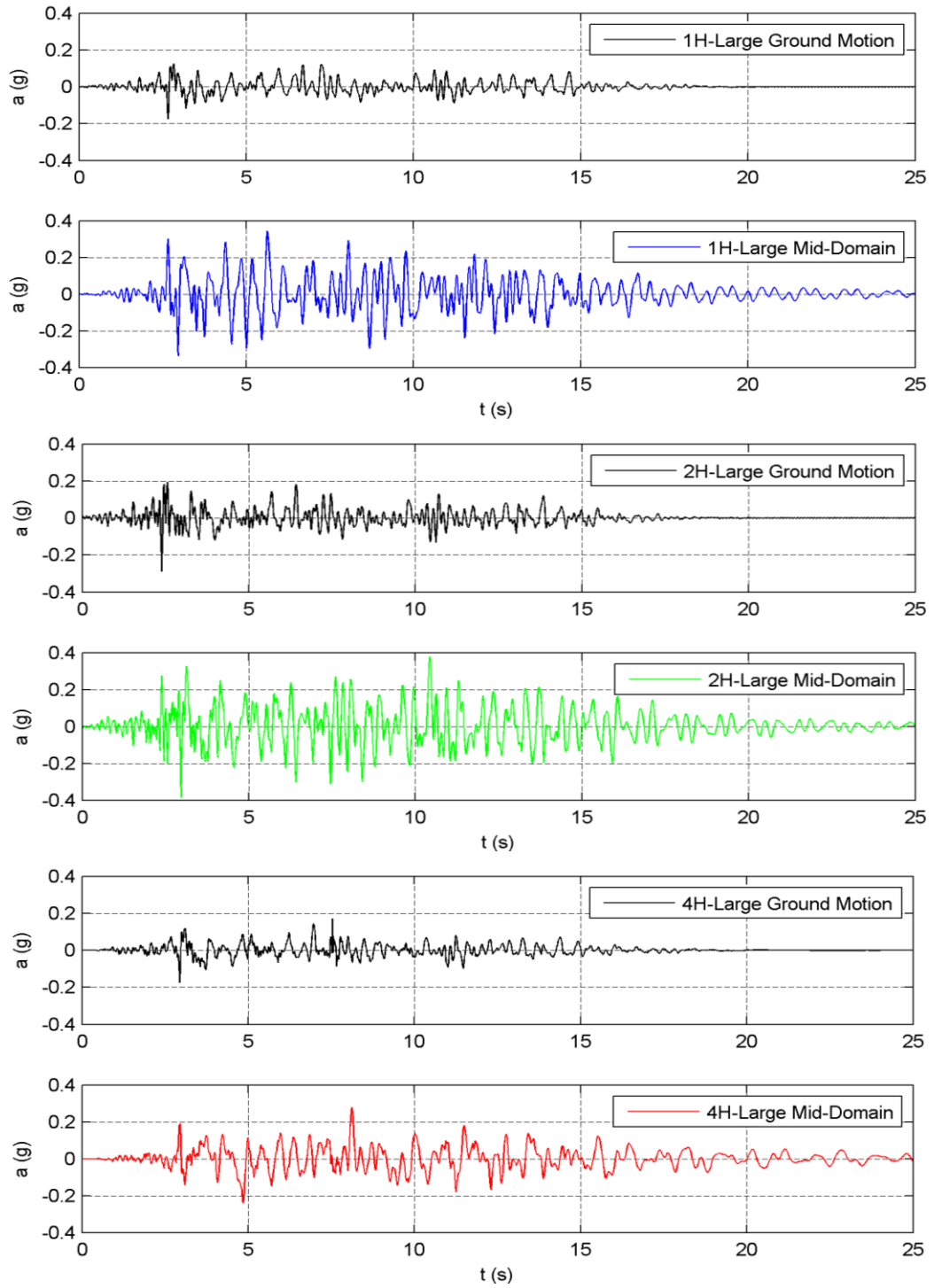
Figure 4.3. *Accelerations on the Model*

4.5.2. Crest Displacements

Crest displacements are obtained for 3 different soil depths. As can be seen from the Figure 4.4, the highest soil depth produces the biggest crest displacement of 36cm and peaks appear at different times as compared to other two soil depths. It can also be said that as the depth increases fluctuations along the graph show a tendency to decrease.
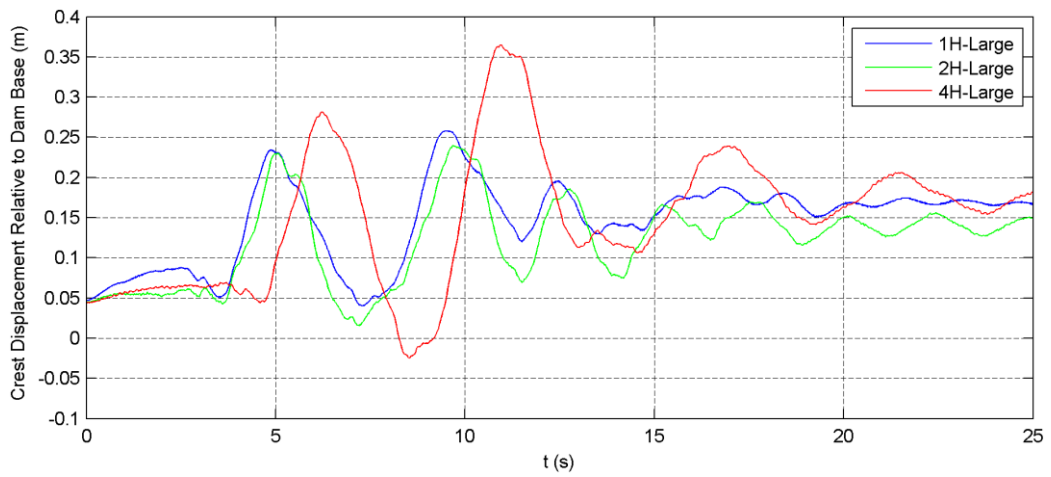
Figure 4.4. *Crest Displacement Relative to Dam Base*

4.5.3. Face slab Axial Stresses

Axial stresses developed in the face slab due to the impounding of water are plotted in Figure 4.5. In general there is no change in the behaviour of the face slab, high tensile stresses peaks within the first 50m then reduces again to a lower level. Most important observation is that as can be seen variation in the soil depth changes the stress state in favor of the face slab.
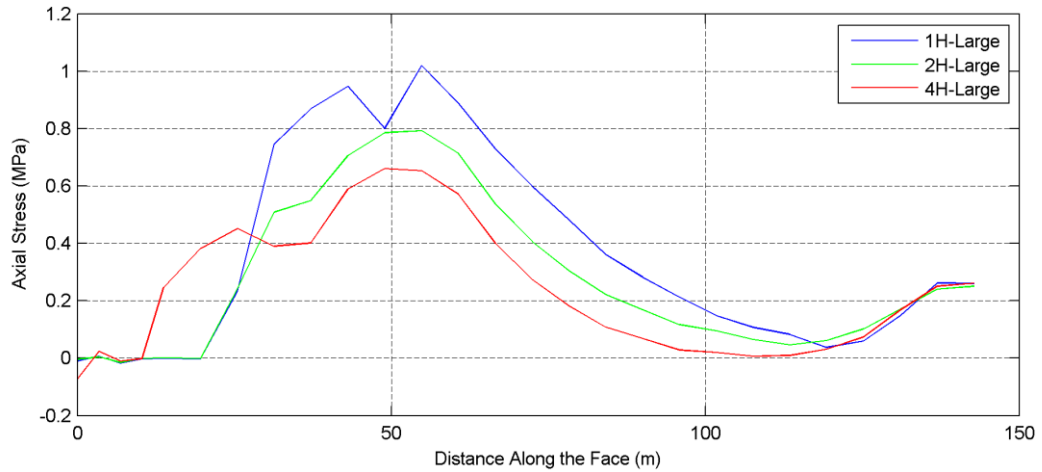
Figure 4.5. *Axial Stresses on the Face Slab*

4.5.4. Face Slab Crack Widths

Face slab crack widths throughout 50cm thick concrete obtained at the end of the impounding and EQ loading are given in Figure 4.6 and Figure 4.7. After the impounding crack widths tend to decrease in size as the model depth increases, although the lower elevations of the face slab shows an adverse tendency. Another remarkable observation is that crackwidth is obtained less along the face place as the model depth increases (Figure 4.6).

After EQ loading cracks at the lower elevations starts to close as the cracks start to spread more along the face slab. Highest width openings shift from low elevations to the middle of the slab. Not so surprisingly, no trend in the performance is observed due to the depth change as the complex dynamic properties start to become more important. Approximate average peak crack widths are observed as 0.8 and 1.7mm for the impounding and EQ loading respectively leading to some possible leakage problems (Figure 4.7).

Figure 4.6. *Crack Widths after Impounding*
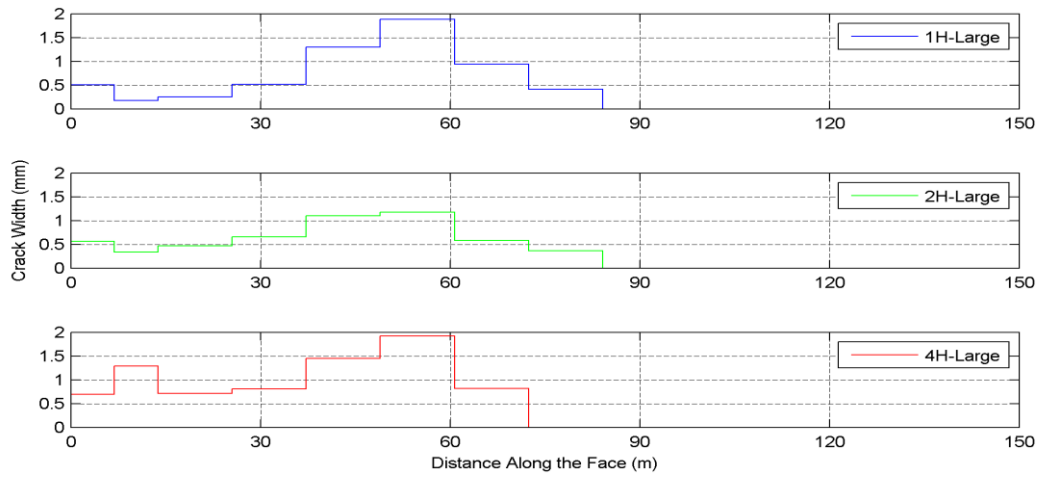
Figure 4.7. Cumulative *Crack Widths after Impoundment and EQ*

CHAPTER 5

SUMMARY AND CONCLUSIONS

5.1. Summary

In the first part of the study, the history of the dam construction is summarized and reasons of the usage of earthly materials in dams are explained briefly. After a brief discussion of the possible failure modes of CFRDs, their advantageous nature as compared to the other dam types are discussed. Previous studies on the SSI effects on the dynamic b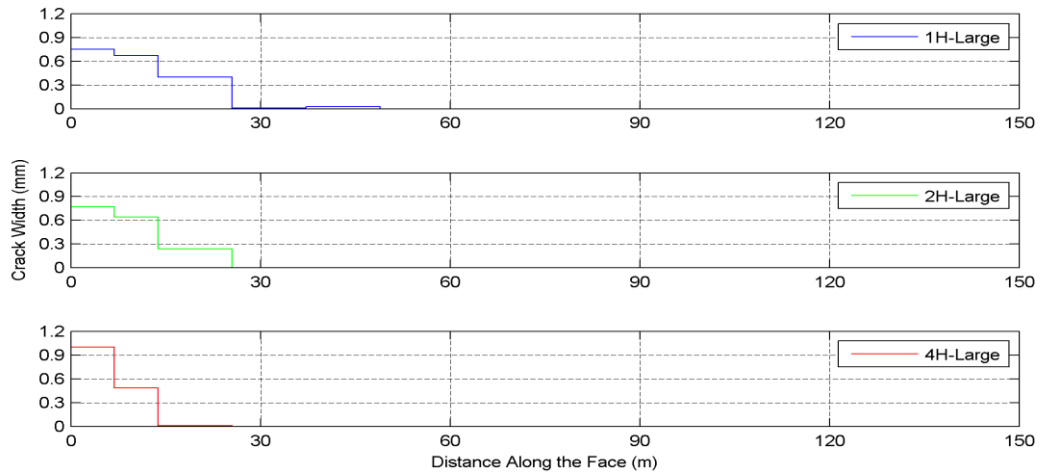ehavior of dams are stated and disadvantages of application of these methods on CFRDs are discussed, mainly considering two important studies conducted by Medina et al. [9] and Fenves & Chopra [8]. Since the main idea of these methods is to simulate the sonic flow correctly, a general description of local boundaries which is created for this task is discussed and the most suitable method is chosen to be applied in the analyses in the rest of the study.

The material models used in the study is presented in the second chapter. These nonlinear material models are used in Chapter 4. The domain size adequate enough to effectively model the impact of SSI is determined in Chapter 3. Model size is determined in a finite element setting by comparing the outcomes of the study to the work by Medina et al. [9] in frequency domain forming the exact model. Since the computational burden to simulate the SSI effects is too high, a well known USACE model [10] is used to approximate the real behavior, accurately represented by the "large" solution, with the proper improvement to the damping and moduli of the model. Success of the model in CFRD application is tested for 3 different

modulus of elasticity values and 3 different soil depths with constant dam geometry; by calibrating the displacement and acceleration results at the crest with the "large" solution values.

In the 4th chapter of the study nonlinear response of a CFRD system is analyzed with the material properties explained in detail in Chapter 2. The main objective of this chapter is to observe the change in response as the soil depth changes (1H, 2H & 4H) when a CFRD is underlain by a weak layer as is typically so for dams placed on valleys with deep alluvium deposits. Acceleration responses at the location of interest, crest displacements, face slab axial stresses and face slab cracks widths are discussed in the related subtopics.

5.2. Conclusions

CFRDs are typically built on stiff alluvium layers which are not excavated during the construction. The SSI effect is usually ignored in the calculations for such systems. The first goal of this study was to investigate the effects of SSI on the response of CFRDs constructed as such. The second goal was to investigate the use of the simplified USACE modeling assumptions for the modeling of the CFRDs given the SSI effects. The final goal of the study was to investigate the crack development on the face slab by taking the effect of SSI and the effect of soil depth change into account. Conclusions in the following paragraphs can be drawn based on the analyses results.

In obtaining the adequate model size to simulate SSI effects, not only the dynamic properties of the system but also the responses in magnitude seem to change drastically depending on the model size. For the first concern, it can said that fundamental frequencies of the systems differ significantly for 10 & 20B models, while 30 & 40B models produce adequate approximations. Similarly, responses of the systems constructed differ significantly for 10 & 20B models, while for the other two models that difference seems acceptable. As a general trend, it is observed that as the frequency of interest gets close to the first fundamental mode of the dam, response of the system produces more error.

In testing the modified USACE model performance, the reduction of the simplified model's soil moduli with an δ factor as the two materials (dam and soil) approach similar stiffness is an expected outcome. Similarly, depending on the soil depth & V_s increase, equivalent damping for the simpler model increases and decreases respectively. However, the modified USACE model yields insufficient performance when the elasticity of the dam approaches the elasticity of the soil, especially due to the increased contribution of the dam's natural vibration modes into the general response. It should also be stated that even if the crest displacement results are accurate enough, acceleration responses produce significantly lower results for frequencies higher than the natural vibration modes, leading to the specification of possible under conservative design loads. So, it is not possible to use such an approach for the analysis of a CFRD if the motion is not dominated by the fundamental mode or low frequency content (i.e. the modulus of elasticity of the two materials are close to each other).

Nonlinear response outcomes point out to an increase in crest displacements during strong ground motion shaking as the soil gets more deep, which may lead to higher strains along the dam body. On the contrary, face slab axial tensile stresses decrease depending on the increase of soil depth during static loading (impounding). As stated previously within the related chapter, approximate crack widths are 0.8 and 1.7 (mm) for impounding and EQ loading respectively. According to ACI [38] for water retaining structures service crack widths should not exceed 0.1 mm. For CFRD's crack widths up to 1.0 mm were deemed adequate [39]. In a situation where it is thought that such limits are critically approached, it is advised to consider an increase the steel ratio in the face slab since the reinforcing steel stress is the most important variable in this cases [40]. If the face slab is not designed properly some treatment can become necessary after construction, if the leakage is not decreased due to clogging [41]. It is also a remarkable observation that after EQ loading crack widths spread more widely along the face slab, almost covering 60-65 % of the total length of the slab.

Finally, it should be stated here that all results presented in the related section of the study are unique to the dam used in the study, especially damping ratios and

Rayleigh parameters. Although the presented conclusions are considered as reliable for all CFRDs, results presented in the related figures may differ.

5.3. Future Work

The future studies that can be carried out based on this work can be summarized as follows:

The effect of reservoir-dam and reservoir-soil interaction should be investigated properly for concrete faced rockfill dams.

The nonlinear response of a concrete faced rockfill dam should be investigated in detail given that excessive cracking was observed in this study. Spreading of the cracking during earthquake loading is an interesting phenomena supported by the increased leakage on the systems after undergoing earthquake shaking.

The effect of modeling assumption and model size on the results should be investigated. As a detailed nonlinear analysis should involve a more refined mesh discretization at points of interest, the modeling approach for such a zone coupled with a coarser mesh for domain effects should be sought.

REFERENCES

1.   Schnitter N. *Verzeichnis geschichtlicher Talsperren bis Ende des 17. Jahrhundert. Historische Talsperren* In G. Garbrecht; p.9-20.

2.   Cooke JB. *Progress in rockfill dams. Journal of Geotechnical Engineering* 1982.

3.   Galloway J. *The design of rockfill dams. Transactions, ASCE* 1939; 104, p. 1-92.

4.   Hirschfield, R. & Poulos, S. *Embankment dam engineering. John Wiley and Sons, Inc* 1972.

5.   Seed HE. *Performance of dams during earthquakes. Journal of the Geotechnical Engineering Division* 1978; 992.

6.   Uddin N. *A dynamic analysis procedure for concrete-faced rockfill dams subjected to strong seismic excitation. Computers and Structures* 1999; p.409-421.

7.   Wieland M. *CFRDs in highly seismic regions. Int. Water Power Dam Consr.* 2010.

8.   Fenves & Chopra [8], G. & Chopra, A.K. *Simplified earthquake analysis of concrete gravity dams:seperate hydrodynamic and foundation effects. Journal of Engineering Mechanics* 1985.

9.   Medina F, Domingues, J. & Tassoulas, J. L. *Response of dams to earthquakes including effects of sediments. Journal of Structural Engineering* 1990.

10.   U.S. Army Corps of Engineers. *Seismic Design Provisions for Roller Compacted Concrete Dams*. 1995.

11.   Kausel E. *Local tranmitting boundaries. Journal of Engineering Mechanics* 1988; 114.

12.   Lysmer, J. & Waas, G. *Shear waves in plane infinite structures. Journal of Engineering Mechanics Division* 1972; 98, p.85-105.

13.   Waas G. *Linear two-dimensional analysis of soil dynamics problems in semi-layered media. Thesis presented to the University of California, Berkeley, at Berkeley, California, in partial fulfillment of the requirements of the degree of Doctor of Philosophy* 1972.

14.   Kausel E. *Forced vibrations of circular foundations on layered media. Department of Civil Engineering, M.I.T.* 1974; p.74-11.

15.   Engquist, B. & Majda, A. *Absorbing boundary conditions for acoustic and elastic wave equations. Mathematics of Computation* 1977; p.629-651.

16.   Lindman EL. *On getting all of the waves out of the box. Journal of Computational Physics* 1975; p.66-78.

17.   Lysmer, J. & Kuhlemeyer, R.L. *Finite dynamic model for infinite media. Engineering Mechanics Division* 1969.

18.   Ang, H. & Newmark, N. *Development of a transmitting boundary for numerical wave motion calculations. Defense Atomic Support Agency* 1972.

19.   Smith WD. *A non-reflecting plane boundary for wave propagation problems. Journal of Computational Physics* 1974; p.492-503.

20.   Liao, Z. & Wong, H. *A transmitting boundary for the numerical simulation of elastic wave propagation. Soil Dynamics and Earthquake Engineering* 1984; p.174-183.

21.   Arici Y. *Investigation of the cracking of the CFRD face plates. Computers and Geotechnics* 2011, 38(7), p.905-916.

22.   TNO DIANA. *TNO DIANA Reference Manual*. 2007.

23.   Varadajaran A, Sharma K, Venkatachalam, K. & Gupta, A. *Testing and modeling two rockfill materials*. *Journal of Geotechnic and Geoenvironmental Engineering* 2003; 30, p.990-1003.

24.   Groen A. *Elastoplastic modeling of sand using conventional model*. *Delft University of Technology* 1995; 03.21.0.31.34/35.

25.   Banerjee N, Seed, H., & Chan, C. *Cyclic behavior of dense coarse grained sands in relation to seismic stability of dams*. *Earthquake Engineering Research Center, Berkeley, California* 1979; 79/13.

26.   Cao X, He, Y. & Xiong, K. *Confining pressure effect on dynamic response of high rockfill dam*. Frontiers of Architecture and Civil Engineering in China 2010; 4(1), p.116-126.

27.   Seed H, Wong R, Idriss, I. & Tokimatsu, K. *Moduli and damping factors for dynamic analysis of cohesionless soils*. Earthquake Engineering Research Center, Berkeley, California 1984; 94/14.

28.   Uesugi M, Kishida, H. & Uchikawa, Y. *Friction between dry sand and concrete under monotonic and repeated loading*. *Soils Found.* 1990; 30(1), p.115-128.

29.   Zhang, G. & Zhang, J. *Numerical modelling of soil-structure interface of a concrete face rockfill dam*. *Computers and Geotechnics* 2009; 36(5), p.762-772.

30.   Vermeer, P. & DeBorst, R. *Non-associated plasticity for soils, concrete and rock*. *Heron* 1984; 29(3), p.3-64.

31.   White W, Valliappan, S. & Lee, I. *Unified boundary for finite dynamic models*. *Journal of Engineering Mechanics Division* 1977; p.949-964.

32.   SAS Ip Inc. *Element Reference for ANSYS 11*. 2007.

33.   Nagtegaal JC, Parks, D.M. & Rice, J.R. *On numerically accurate finite element solutions in the fully plastic range*. *Computer Methods in Applied Mechanics and Engineering* 1974.

34.   NEHRP Recommended Provisions for Seismic Regulations for New Buildings and Other Structures. 2003; FEMA 450.

35.   Cooke, J.B. & Sherard, J.L. *Concrete Face Rockfill Dams-Design, Construction and Performance.* Proceeding of a symposium sponsored by the geotechnical engineering division of ASCE. 1985.

36.   Hunter, G. & Fell, R. *Rockfill modulus and settlement of concrete face rockfill dams. Journal of Geotechnical and Geoenviromental Engineering, ASCE* 2003; 123.

37.   Gergely, P. & Lutz, L.A. *Maximum crack width in reinforced concrete flexural members. American Concrete Institute* 1968; SP-20 (Causes, Mechanism, and Control of Cracking in Concrete), p.87-117.

38.   ACI Committee 318. *Building Code Requirements for Structural Concrete and Commentary 2005. American Concrete Institute* 2005.

39.   Haselsteiner, A. & Ersoy, B. *Seepage control of concrete faced dams with respect to surface slab cracking.* 6th International Conference on Dam Engineering 2011.

40.   ACI Committee 224. *Control of Cracking in Concrete Structures 2001. American Concrete Institute* 2001.

41.   Fitzpatrick MD, Cole BA, Kinstler, F.L. & Knoop, B.P. *Design of concrete faced rockfill dams. Journal of Geotechnical & Geoenvironmental Engineering* 1987; 113 (10), p.410–434.